FOI-R--1309--SE
February 2005
ISSN1650-1942

Technical report

Hagfors Seismic Array Performance Analysis

Björn Lund and Malin Lennartsson

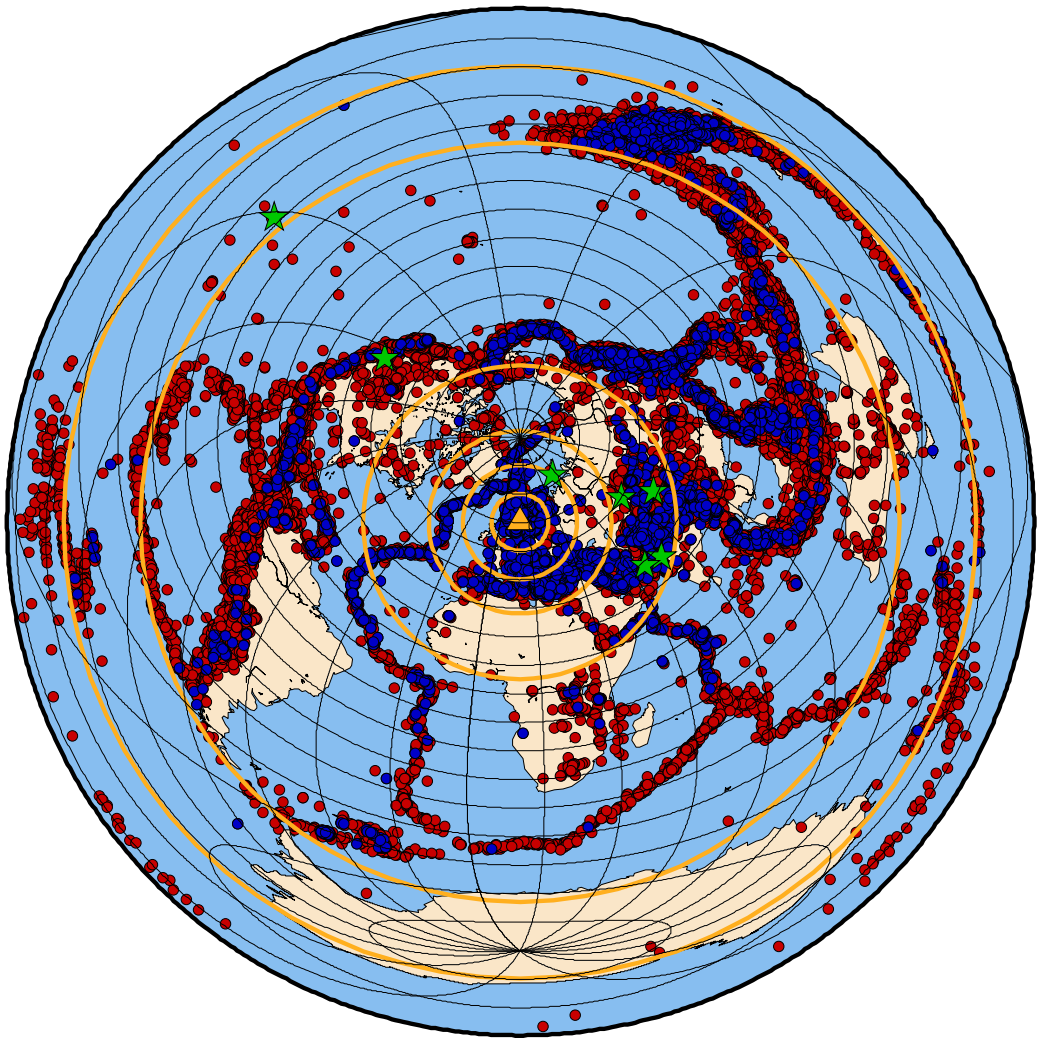

Division of Systems Technology
SE-172 90 STOCKHOLM
Sweden

Swedish Defence Research Agency
Division of Systems Technology
SE-172 90 STOCKHOLM
Sweden

FOI-R--1309--SE
February 2005
ISSN1650-1942

Technical report

Hagfors Seismic Array Performance Analysis

Björn Lund and Malin Lennartsson

Issuing organization

Swedish Defence Research Agency
Division of Systems Technology
SE-172 90 STOCKHOLM
Sweden

Report number, ISRN
FOI-R--1309--SE

Report type
Technical report

Research area code
3. NBC Defence and other hazardous substances

Month year
February 2005

Project no.
A69011

Sub area code
34 International Security

Sub area code 2

Author/s (editor/s)

Björn Lund and Malin Lennartsson

Project manager
Leif Persson

Approved by
Monica Dahlén

Sponsoring agency
Ministry for Foreign Affairs

Scientifically and technically responsible
Leif Persson

Report title

Hagfors Seismic Array Performance Analysis

Abstract

The Hagfors seismic array was modernized during the summer of 2001. New subsurface vaults, cables and instruments were installed and the array was operational on April 5, 2002. During the period 5/4-2002 to 21/9-2003 the old and new Hagfors arrays operated in parallel. Here we report on a variety of measurements and parameters related to the operation and performance of the two arrays. Included is array configuration details, instrument and array noise studies and array gain and response calculations. Using NORSAR's single array processing we have compared the performance of the two arrays on a regional scale. We have also studied the results of the two array's participation in the CTBTO IDC processing on a global scale.

Keywords

Seismology, monitoring testban treaty, seismic array station, array analysis, regional- and teleseismic event analysis

Further bibliographic information

Language
English

ISSN
1650-1942

Pages
48

Distribution

By sendlist

Price Acc. to pricelist

Security classification Unclassified

Utgivare

Totalförsvarets forskningsinstitut
Avdelningen för Systemteknik
SE-172 90 STOCKHOLM
Sweden

Rapportnummer, ISRN
FOI-R--1309--SE

Klassificering
Teknisk rapport

Forskningsområde
3. Skydd mot NBC och andra farliga ämnen

Månad, år
Februari 2005

Projektnummer
A69011

Delområde
34 Internationell säkerhet

Delområde 2

Författare/redaktör

Björn Lund and Malin Lennartsson

Projektledare
Leif Persson

Godkänd av
Monica Dahlén

Uppdragsgivare/kundbeteckning
Utrikesdepartementet

Tekniskt och/eller vetenskapligt ansvarig
Leif Persson

Rapportens titel

Utvärdering och analys utav Hagfors seismiska array

Sammanfattning

Under sommaren 2001 gjordes en modernisering av Hagfors seismologiska array. Nya underjordiska kammare, nya kablar och instrument installerades och arrayen var i full drift 5 april 2002. Under de första 18 månaderna (5/4-2002 till 21/9-2003) var både gamla och nya arrayen i drift parallellt. Denna rapport innehåller mätningar och parametrar som relaterar till driften och prestandan av de två arrayerna. Inkluderat är arraykonfigurationer och instrument, brus-studier, arrayrespons och gainberäkningar. Med hjälp av NORSARs array processering för enstaka arrayer har de två arrayernas prestanda jämförts på regional nivå. De två arrayernas medverkan i CTBTO IDC globala processering har också studerats.

Nyckelord

Seismologi, provstoppsövervakning, mätstation, arrayanalys, regional- och teleseismisk analys

Övriga bibliografiska uppgifter

Språk
Engelska

ISSN
1650-1942

Antal sidor
48

Distribution

Enligt missiv

Pris Enligt prislista

Sekretess Öppen

Contents

1 Introduction **7**

2 Array configuration and instrumentation **8**
2.1 Element spacing . . . 9
2.2 Azimuthal variation in the spatial extent of the two Hagfors arrays . . . 9
2.3 Instrumentation and signals . . . 9
2.4 Array respons . . . 13

3 Noise studies **14**
3.1 Signal energy . . . 14
3.2 Power spectral densities . . . 14
3.3 Noise correlation . . . 16
3.4 Summary of noise studies . . . 18

4 Signal studies **19**
4.1 Signal correlation . . . 19
4.2 Gain . . . 20
4.3 The Kazakhstan field experiment . . . 23
4.4 Summary of signal studies . . . 24

5 Event analysis at Hagfors **25**
5.1 IDC processing and the REB . . . 25
5.1.1 Hagfors data in the REB . . . 26
5.1.2 Azimuth and slowness residuals . . . 27
5.1.3 Summary . . . 30
5.2 EP processing at NORSAR . . . 31
5.2.1 EP statistics . . . 31
5.2.2 Comparison with the NORSAR regional reviewed bulletin . . . 34
5.2.3 Comparison with the SNSN bulletin . . . 39
5.2.4 Summary . . . 40

6 Software **41**

7 Summary and discussion **43**

Acknowledgments **43**

References **44**

Appendices: **45**

A Sensitivities for sensors and digitizers in the new and the old array **45**

B Hagfors REB events for various regions **46**

C EP-processing issues **47**

1 Introduction

The Hagfors seismic array station was established 10 km north of Hagfors, see map in Fig. 1, in the late 1960s. It has been operated by the Swedish Defence Research Agency FOI since the start and the most recent of the technical upgrades of the station, performed during the summer of 2001, provides the basis for this report.

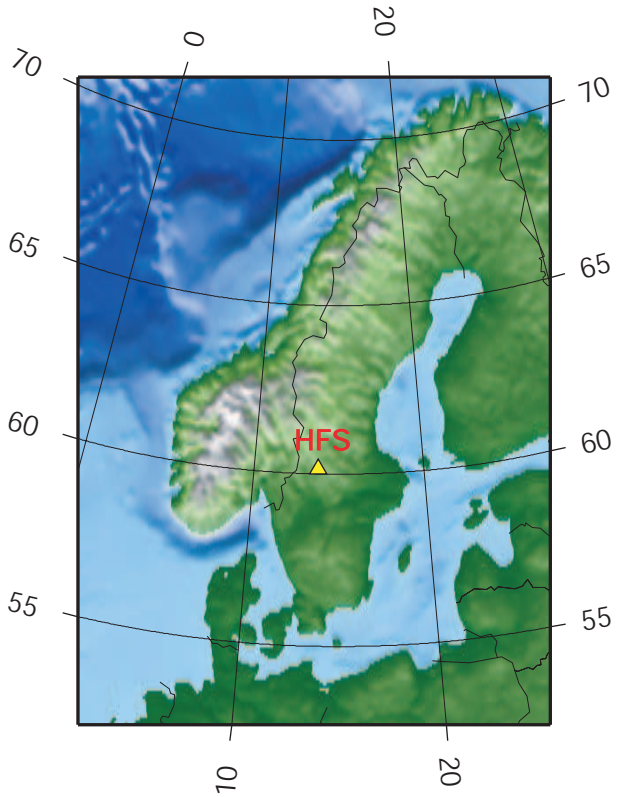

Figure 1: Map showing the location of the Hagfors seismic array station

The Hagfors array has been designated as facility AS101 of the auxiliary seismic station network of the International Monitoring System (IMS), to be established under the Comprehensive Nuclear-Test-Ban Treaty (CTBT). The station is also a temporary substitute for primary seismic stations in Europe and West Asia (CTBT/PC-10/1/Annex II/Appendix IV). Due to deteriorating infrastructure and aging and heterogeneous instrumentation, the array was completely refurbished in 2001. The number of array elements were increased from eight to ten, new element sites were constructed, new communication and power cables were laid down and new instruments and a new data acquisition system installed. Data communication to the International Data Center (IDC) of the Comprehensive Nuclear-Test-Ban Treaty Organization (CTBTO) is provided through a direct satellite link. Hagfors data is currently transmitted to the Swedish National Data Center (NDC) at FOI via a satellite link to NORSAR, a Norwegian seismic research center and the location of the Norwegian NDC, and then forwarded from Norway over the Internet.

The upgrade of the Hagfors array was completed on April 5, 2002. Since the array was completely rebuildt, it was possible to keep the old array running during the construction of the new array, and we decided to continue operation of the old array for some time after the completion of the new array. The two arrays, therefore, operated in parallel approximately one and a half year (April 5, 2002, to September 21, 2003). This provided us with an excellent opportunity to compare the performance of the two arrays on the same events and external conditions.

This report provides a broad overview of a number of seismic array related issues and is also a snapshot of array performance during the studied time period, which extends from January 1, 2000, through the period of simultaneous operation up until February, 2004. We study topics such as Hagfors participation in the IDC event definition, array gain and signal-to-noise ratios. We also compare array characteristics and processing results for the new and the old array in areas such as noise levels, signal coherency and azimuth and slowness residuals. The study identifies some peculiarities and problems which require further investigations in order to complete the analyses.

2 Array configuration and instrumentation

The geographic locations of the elements in the old, eight element, and the new, ten element, arrays are shown in Fig. 2 and Table 1. The new Hagfors array is constructed using the concentric ring approach, with a central element and two rings. The inner A-ring has three elements and the outer B-ring has five elements. In addition, there is an element, C2, south of the ring. The diameter of the outer ring is approximately 1.4 km. The old array had a central element with a single circle of five elements surrounding it, plus two elements outside the ring to the south. The ring diameter was approximately 900 m.

Element	Latitude	Longitude	Altitude (km)
HFA0	60.141965	13.684988	0.2749
HFA1	60.144449	13.684584	0.2945
HFA2	60.140567	13.680606	0.3019
HFA3	60.140466	13.689584	0.2659
HFB1	60.148188	13.682351	0.3238
HFB2	60.142126	13.672940	0.3417
HFB3	60.137039	13.682041	0.2719
HFB4	60.138456	13.694303	0.2662
HFB5	60.146693	13.696394	0.2537
HFC2	60.133474	13.694490	0.2967
HFSA1	60.137314	13.692697	
HFSB1	60.137192	13.699025	
HFSB2	60.142344	13.696067	
HFSB3	60.142428	13.685544	
HFSB4	60.137483	13.681958	
HFSB5	60.134158	13.690706	
HFSC1	60.133558	13.694253	
HFSC2	60.132569	13.695756	

Table 1: Coordinates of the new (upper, HF coded) and the old (lower, HFS coded) element sites in the Hagfors arrays. The coordinates are given in the WGS84 reference system.

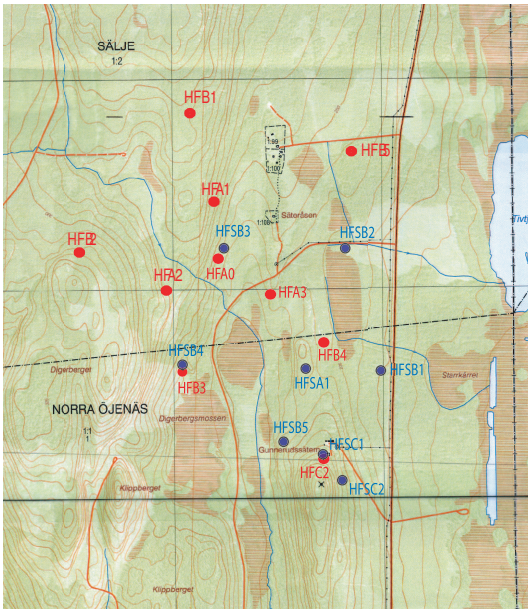

Figure 2: Map showing the old (blue dots) and the new (red dots) arrays.

2.1 Element spacing

Before the installation of the new array some estimations were made with the old array for array-configuration optimization [1]. Similar analyses have been carried out earlier, e.g. for NORSAR's NORESS array [3] and an earlier version of the Hagfors array [2].

Noise cross-correlation studies at different element separations with the old array gave negative correlation in the frequency band 2-5 Hz for distances between 500 and 1000 m. Therefore the new array was built with several intra-array spacings between 500 and 1000 m (see Figure 3). Unfortunately the new array lost the smallest spacing less than 300 m. The 10 elements in the new array gives 45 intra-array spacings between 300-1800 m. The old arrays 8 elements gave 28 spacings between 100-1200 m.

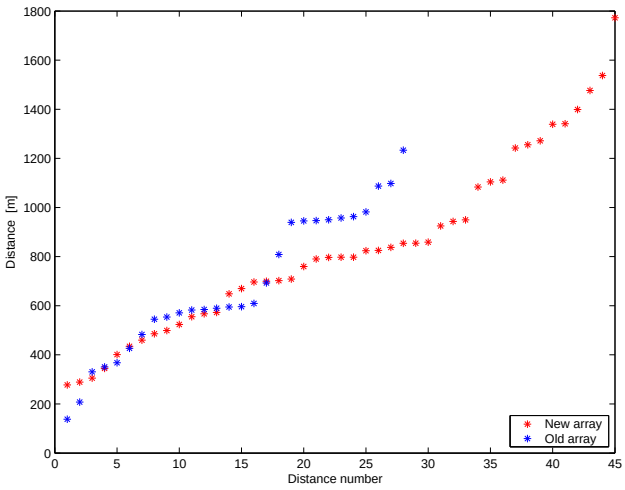

Figure 3: Intra-array spacings, 45 in total for the 10 elements in the new array and 28 for the 8 elements in the old array.

2.2 Azimuthal variation in the spatial extent of the two Hagfors arrays

In order to more emphasize the difference in the extent of the old and the new Hagfors arrays, we calculated the apparent size of the array seen by waves incoming from different azimuths. For each 1° in azimuth we projected the array elements onto the ray path and calculated the length from the first encountered element to the last. Similarly, the width of the array can be calculated for each azimuth (this is obviously just a 90° phase shift from the length). In Fig. 4 we show both the array geometry, with a red enclosure that represents the length of the array at different azimuths, and the length/width of the array at different azimuths. We see from Fig. 4 that the new array is significantly larger than the old array, note the different scales, ranging from 1260 - 1770 m in length as compared to 900 - 1250 m for the old array. It is, however, interesting to note that the azimuthal properties of the two arrays are very similar, with the longest apparent length at 150° - 160°. Apparent length and width of the array translates directly to resolution in terms of azimuth and slowness estimates, i.e. the new array has maximum slowness resolution for rays arriving at 155° (and 335°) and maximum azimuth resolution for rays at 65° (and 245°). In Fig. 4 we have denoted the azimuths to some areas of special interest. Table 2 defines the abbreviations used in Fig. 4.

2.3 Instrumentation and signals

The old array consists of both short-period and long-period seismometers from Geotech Instruments and one vertical broadband seismometer from Streckeisen (see Appendix A).

The new array consists of nine short-period seismometers (GS-13) from Geotech Instruments, for specifications and sensitivities see Appendix A, and one three-component broadband seismometer (STS-2) from Streckeisen. The GS-13 has a frequency range from 1 to 50 Hz and STS-2 between 120s and 50 Hz. At each site is one preamplifier and a digitizer installed. The sampling frequency is 80 Hz for the new array and 40 Hz for the old.

Unfiltered data from both the new and the old arrays are shown in Figure 5 and 6. It is only the amplitude that differs between the two arrays. This is also obvious with the event in Värmland region, shown in Figure 7 and 8.

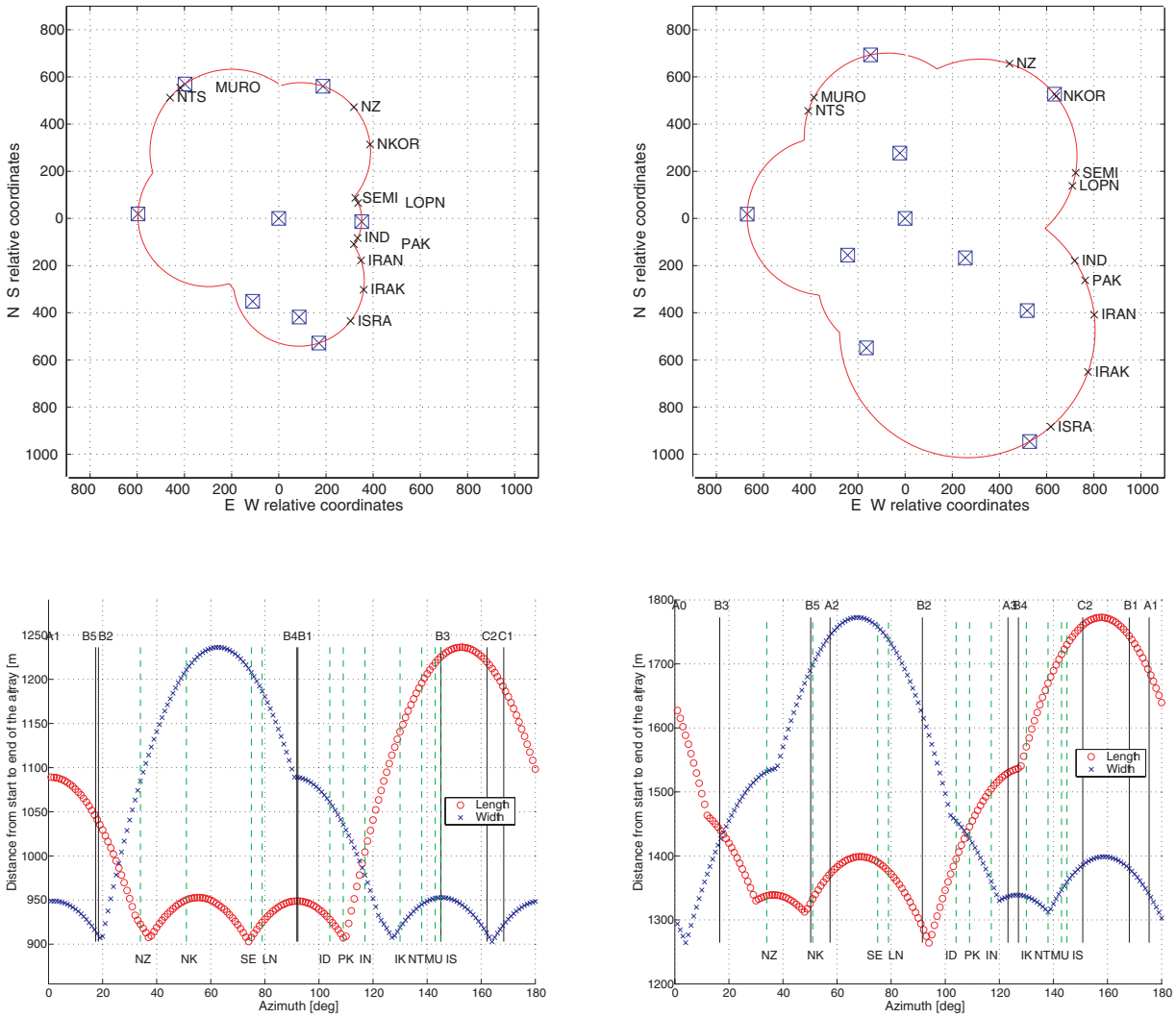

Figure 4: Upper left) Geometry of the old Hagfors array. The blue squares are the array elements, the red line represents the apparent extent of the array seen by a plane wave incoming from a certain azimuth. Abbreviated names are of places of special interest, see the text. Lower left) Length, red, and width, blue, of the array as seen by a plane wave incoming from a certain azimuth. Black lines represent the azimuths of the array elements, folded into 0°-180°, the green dashed lines are back-azimuths to places of special interest, see the text. Upper and lower right show similar plots for the new Hagfors array.

Area	Longitude	Latitude	Back-azimuth from HFS
Novaja Zemlja, Russia (NZ)	55	73	34
North Korea (NK)	126	40	51
Semipalatinsk, Kazakhstan (SE)	78	50	76
Lop Nor, China (LN)	89	42	77
Pokhran, India (ID)	72	27	104
Chagai, Pakistan (PK)	65	29	109
Iran (IN)	54	34	117
Iraq (IK)	43	34	131
Israel (IS)	35	30	145
NTS, USA (NT)	-116	37	320
Muroroa, France (MU)	-139	-22	321

Table 2: Location and back-azimuth, from the HFS reference point, for some nuclear weapon test sites and for some countries that have not signed the Nonproliferation of Nuclear Weapons Treaty (NPT).

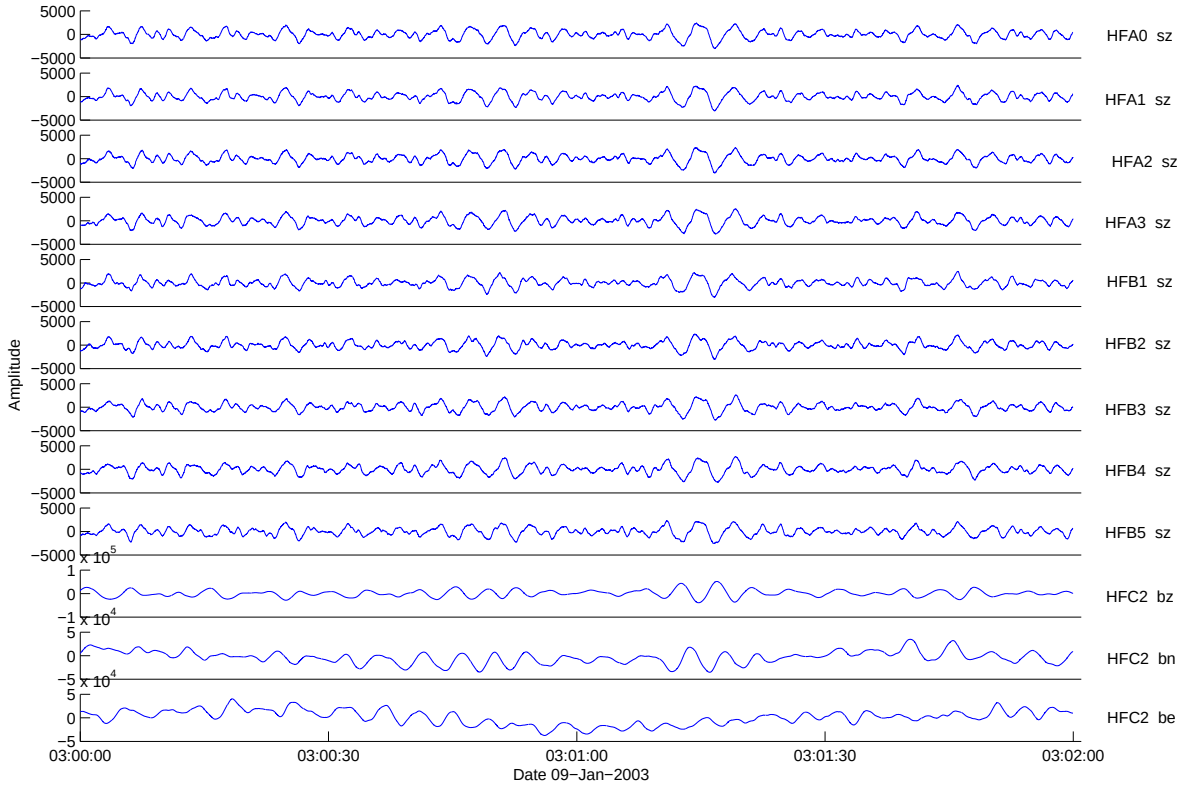

Figure 5: Recorded noisedata from the **new** array from January 9, 2003. Amplitude in counts on the y-axis and time on the x-axis.

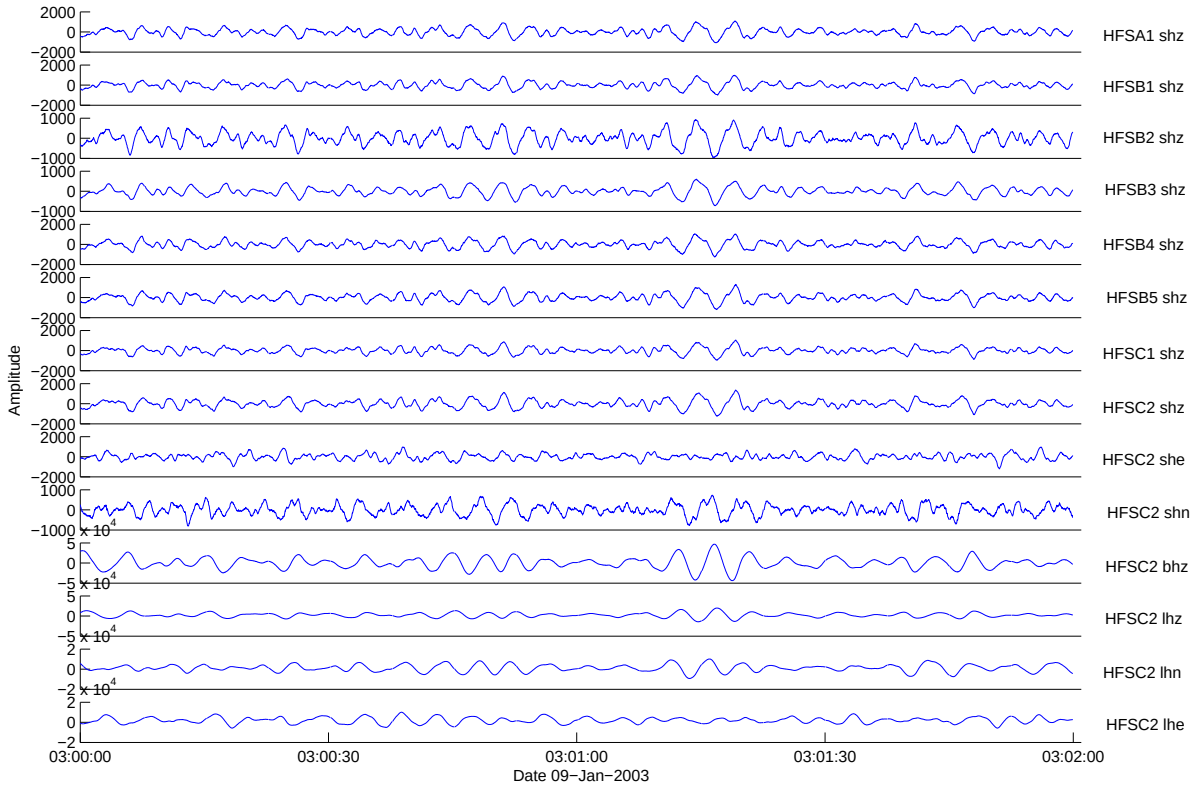

Figure 6: Recorded noisedata from the **old** array from January 9, 2003. Amplitude in counts on the y-axis and time on the x-axis.

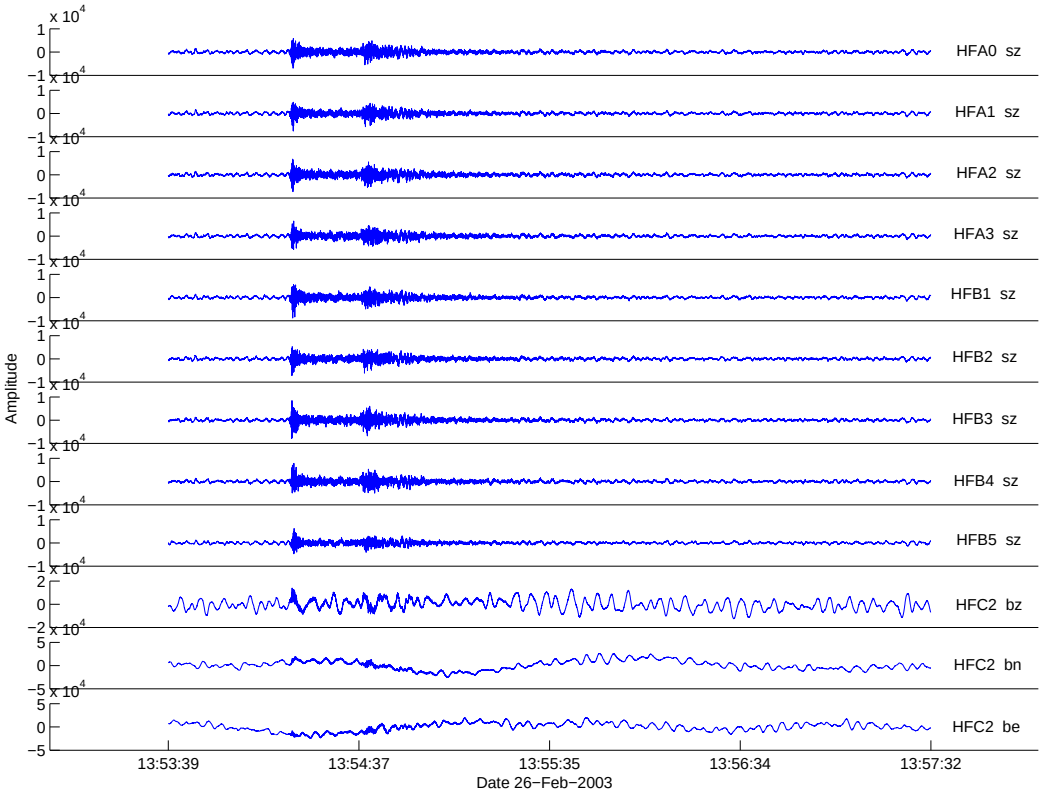

Figure 7: Recorded data from all channels in the **new** array from a local event in February 26, 2003

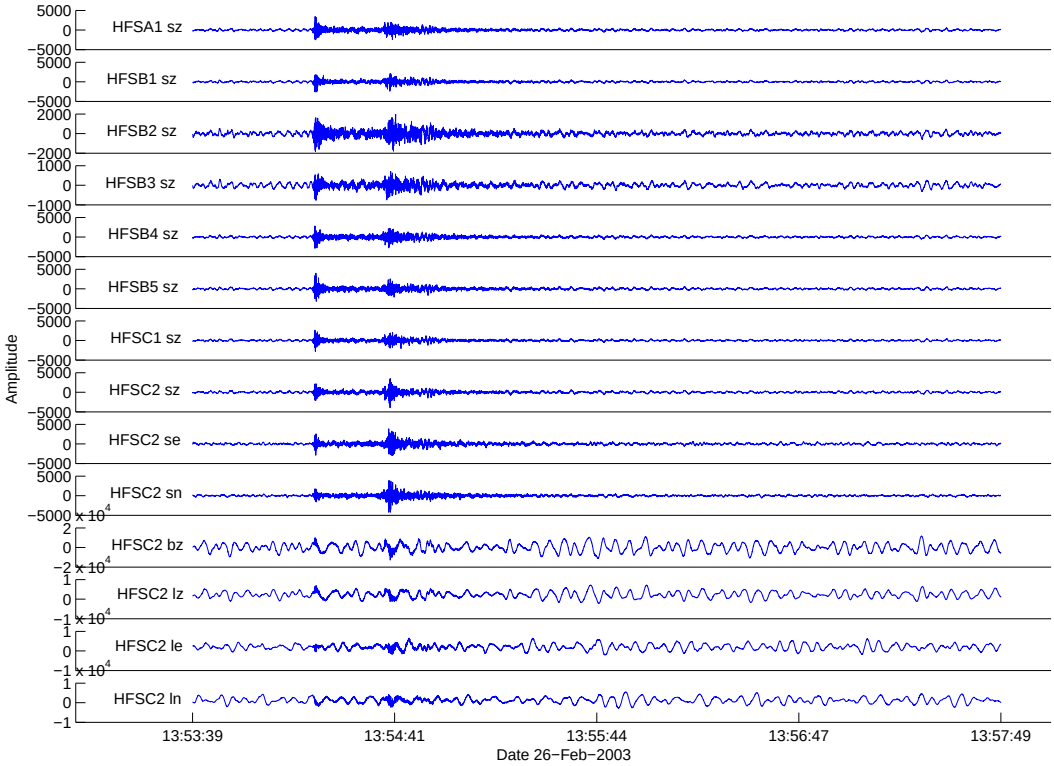

Figure 8: Recorded data from all channels in the **old** array from a local event in February 26, 2003

2.4 Array respons

We have calculated the array responses for the old and the new Hagfors array configurations. The array response provide information on the array's ability to resolve signals from different directions and slownesses. Ideally, we would like an array to have an equally good capability for detecting and measuring signals from all over the Earth. Such an array will have a circular shaped array response pattern with a sharp peak. Another issue for an array is to avoid so-called aliasing effects, which show up as several peaks in the array response pattern.

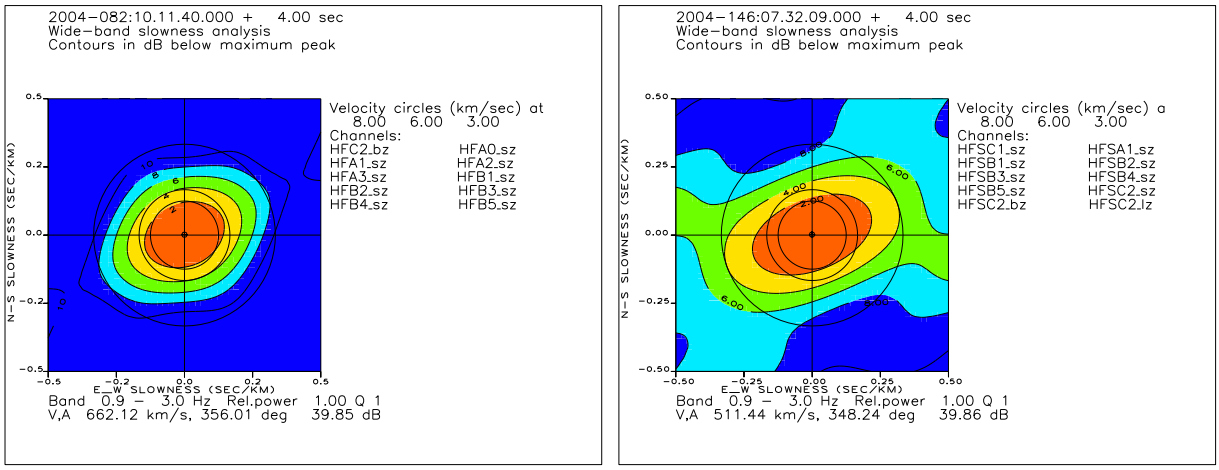

Figure 9: Array-respons for the new (left) and old (right) array. Black isolines are plotted at -2, -4, -6, -8 db below the maximum of the array respons.

The new array has an elliptical NE-SW array response. Looking at the map in Figure 2 we see that the array-sites are located in an NW-SE directed ellipse, which gives us good slowness resolution in NW-SE direction and good azimuth resolution in NE-SW. The old array response (see Figure 9) is located in the same direction as the new array but the uncertainty is larger. So the azimuth and slowness residuals should decrease for the new array as compared to the old one. In conclusion, we find that the new Hagfors array has a sensor configuration and associated array response that make it very capable for detecting and estimating the characteristics of high-frequency signals from all directions and slownesses.

3 Noise studies

3.1 Signal energy

One measure of the energy of the data can be calculated from:

$$E = \frac{1}{N}\sum_{n=1}^{N}(Sig(n) - \hat{Sig})^2$$

where N is the length of the time-window (i.e. 80 samples) and $\hat{Sig}$ is the corresponding mean-value of the signal in the window. The median-value of the energy for 10 minutes of noise data from six quiet days and nights in the beginning of 2003 is displayed in Figure 10. The noise-level varies from one day to another. Site A3 and B4 show slightly higher noise-levels than the rest of the array in both the days and the nights, but the difference between two days is much greater than the difference between two sites at the same day.

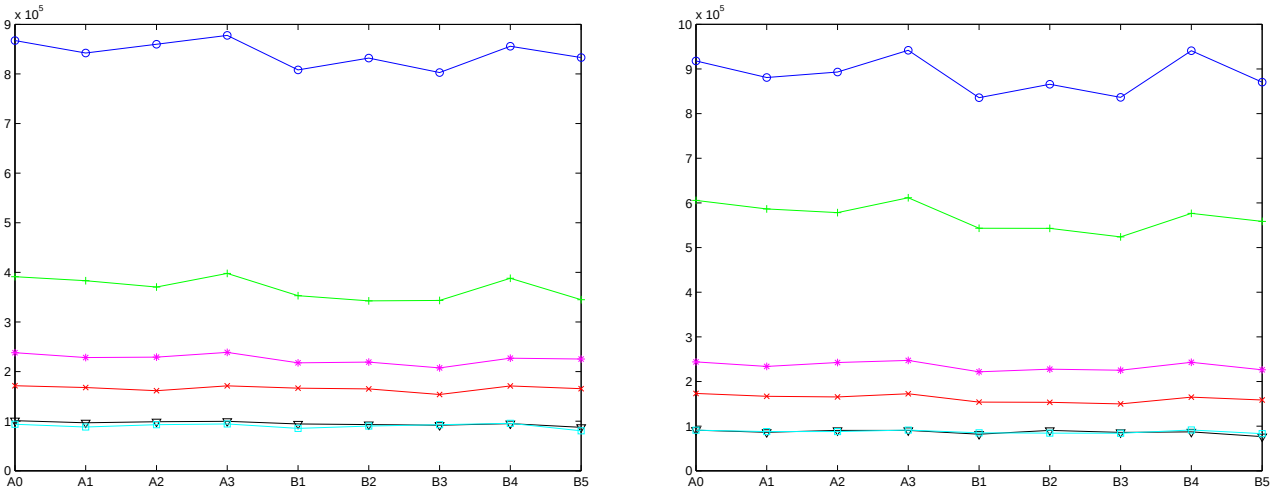

Figure 10: Median values for the new array in day- (left figure) and nighttime (right figure), different color representing different days (red is 20030109, blue is 20030116, green is 20030125, magenta is 20030209, black is 20030222 and cyan is 20030303). Energy on the y-axis and site on the x-axis.

3.2 Power spectral densities

Power spectral densities are estimated for the new and the old arrays, from a night in August 2003, and displayed in Figures 11 and 12. From the short-period seismometers is a data window of 100 s used and from the broadband seismometer 1000s. The data is from the same time for the new and the old arrays. The red lines in the figures are the 'New High Noise Model' (NHNM) and 'New Low Noise Model' (NLNM), representing the upper and lower mean value for seismic noise from the whole world. Both arrays are lower than the NLNM for higher frequencies (>1Hz), indicating that Hagfors is a "quiet" area.

The median-value of the spectrum for all channels is displayed with green in Figure 13. The median-value of the spectrum is showing a low noise-level.

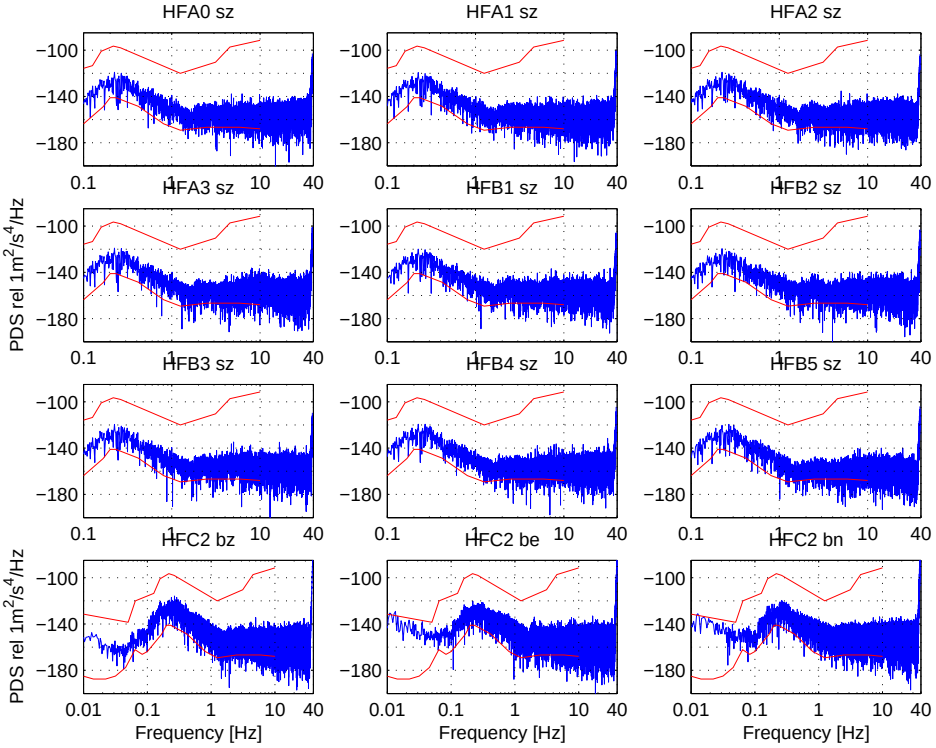

Figure 11: Power spectral densities (dB relative to 1 $m^2/s^4/Hz$) from the **new** array.

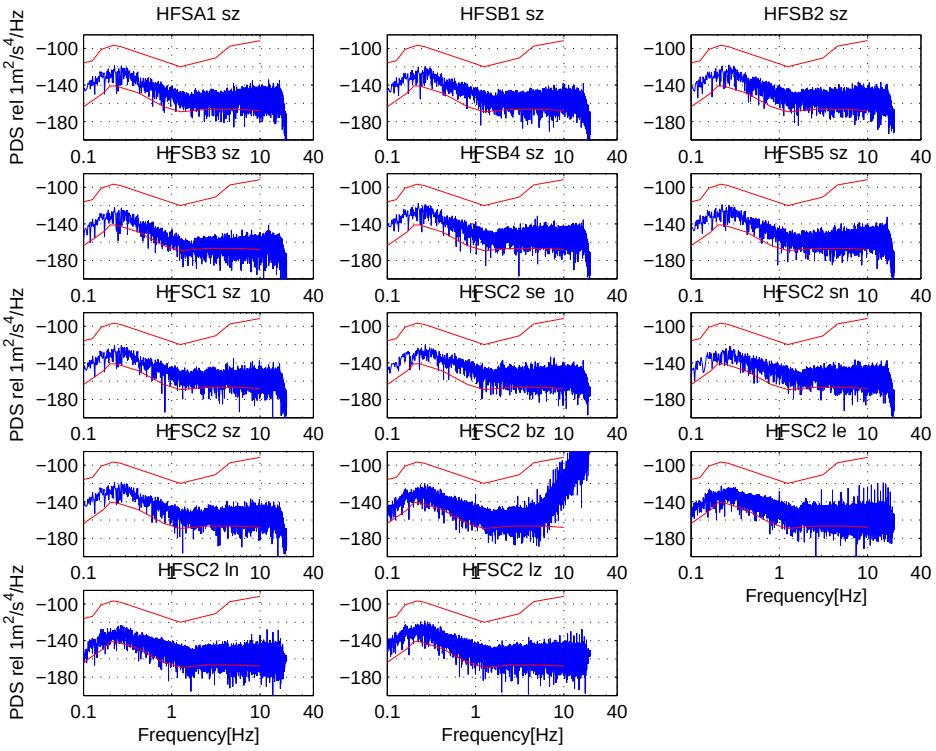

Figure 12: Power spectral densities (dB relative to 1 $m^2/s^4/Hz$) from the **old** array.

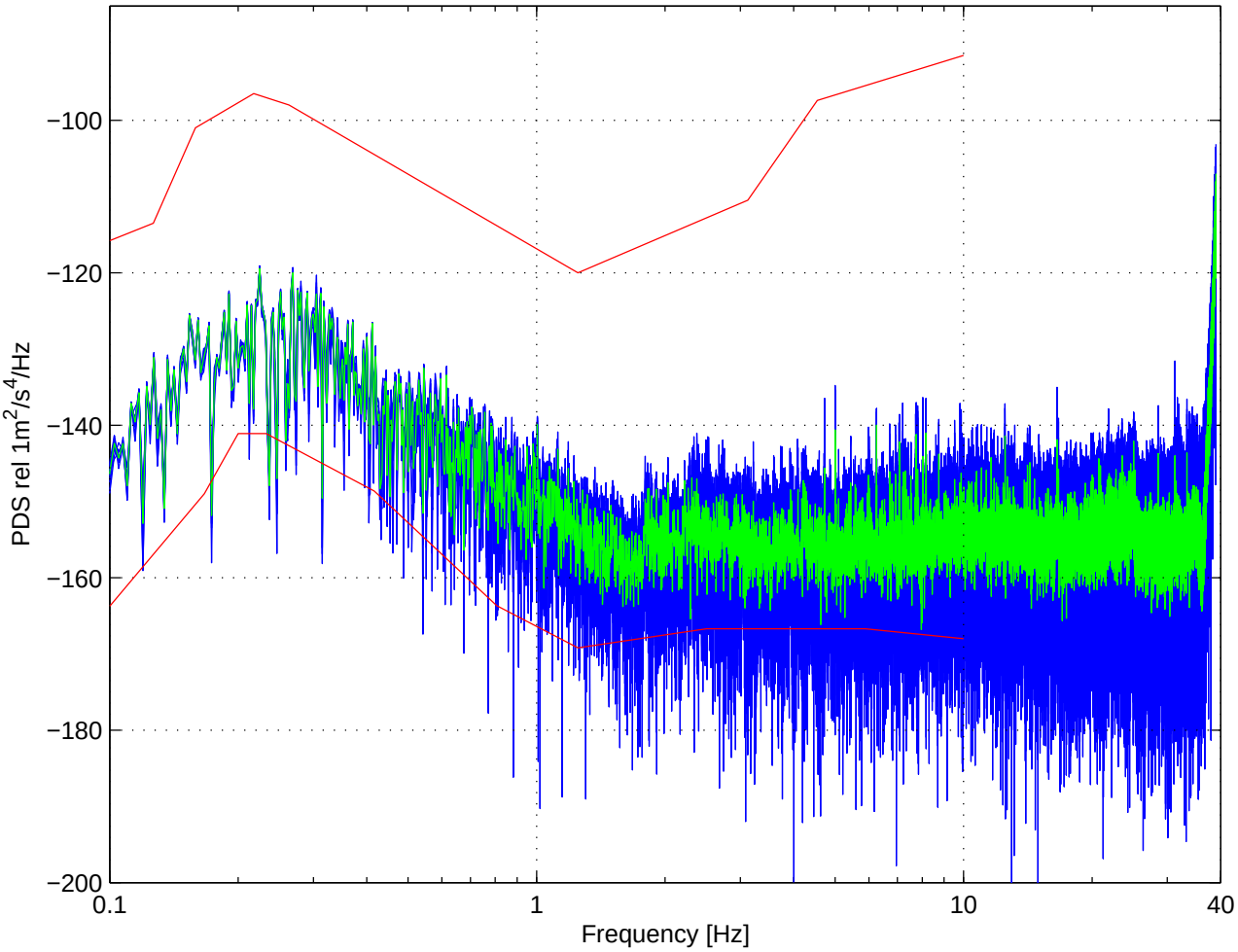

Figure 13: Spectrum of all channels in blue and median spectrum in green for the new array.

3.3 Noise correlation

Cross-correlations between all channels (two channels at a time) were calculated for six days and nights during the winter of 2003. The data contains only noise and is arbitrarily chosen so the noise-levels varies between the days (see Figure 10). The data is taken from the same time instant for both the old and the new array. All datasets are 10 minutes long. The cross-correlations were made with zero-lag for different filter-band, see Figures 14 - 17. 1 in the figure means perfect correlation. The median-value of the cross-correlations for the six days or nights are smoothed with a 3-points average ($x = \frac{x_{n-1}+x_n+x_{n+1}}{3}$) and displayed in red on top of all cross-correlation values (see Figures 14 - 17).

The noise cross-correlation for the new array shows, for both days and nights, that the noise correlates relatively well for low frequencies at shorter distances. The negative correlation, that was found for the old array (see Reference [1]), can be seen for distances between 600 and 1200 for frequency-band 2-3 Hz. In the 3-4 Hz frequency-band the negative correlation shows up both between 300-700 m and between 1200 and 1400 m. The old array does not have the long intra array spacings, over 1200 m, so it shows just the negative correlation between 600-1200 for 2-3 Hz and 300-700 m for 3-5 Hz (see Figures 16 - 17).

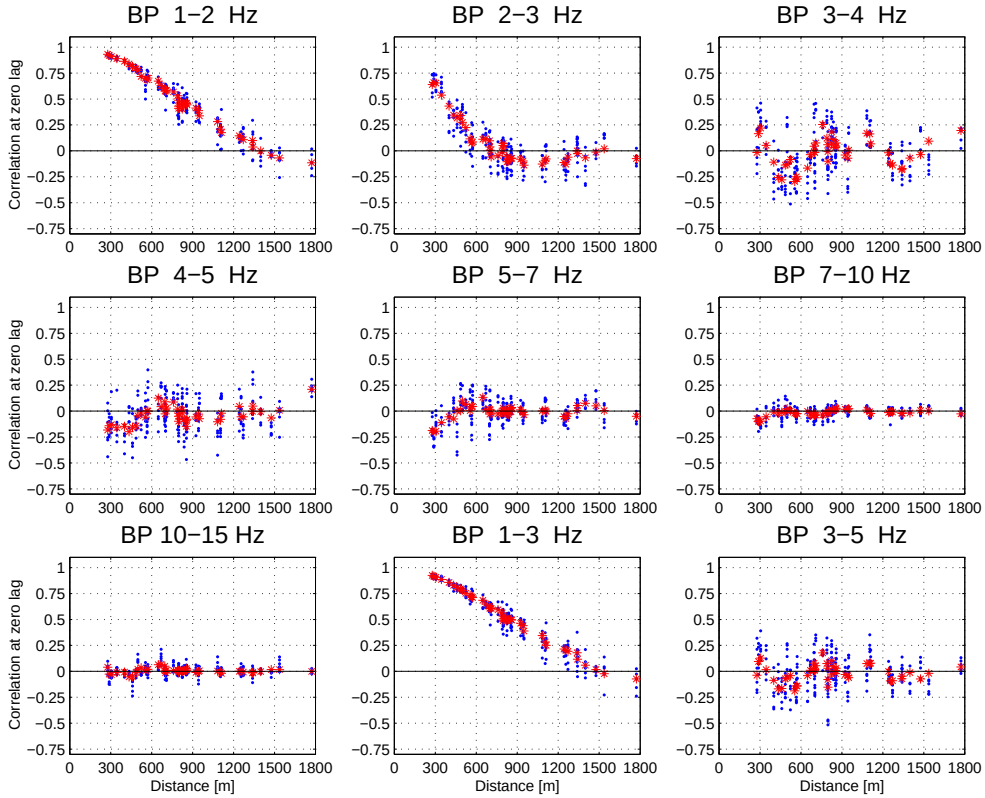

Figure 14: Median-value on top of all values for the cross-correlation for the **new** array at night time.

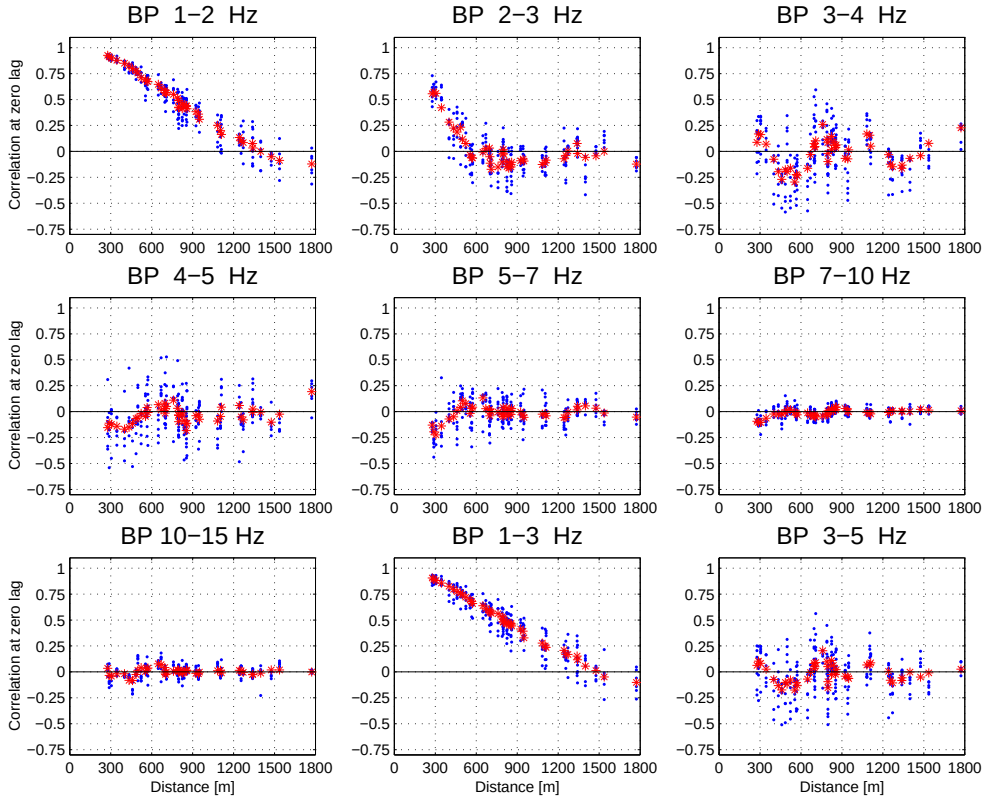

Figure 15: Median-value on top of all values for the cross-correlation for the **new** array at day time.

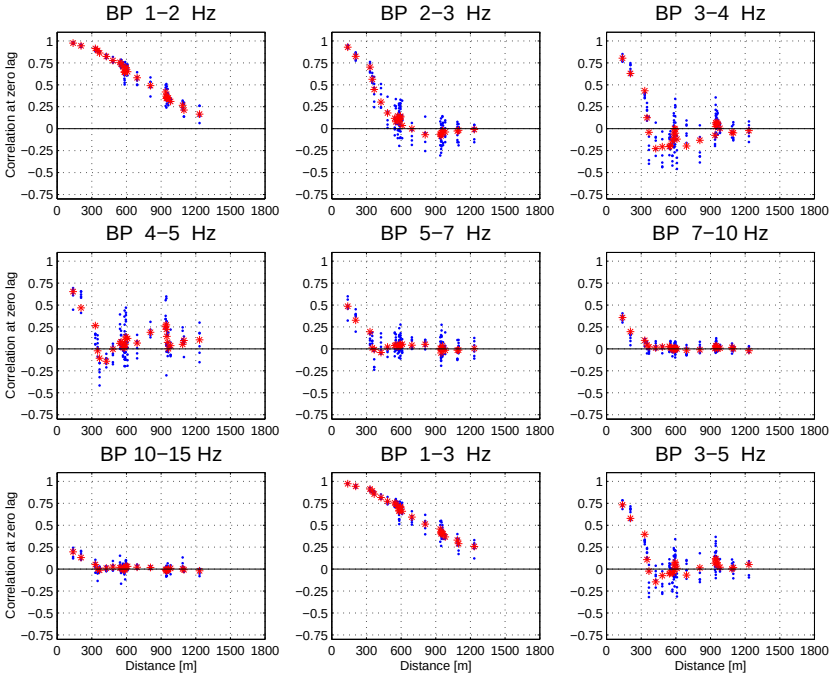

Figure 16: Median-value on top of all values for the cross-correlation for the **old** array at night time.

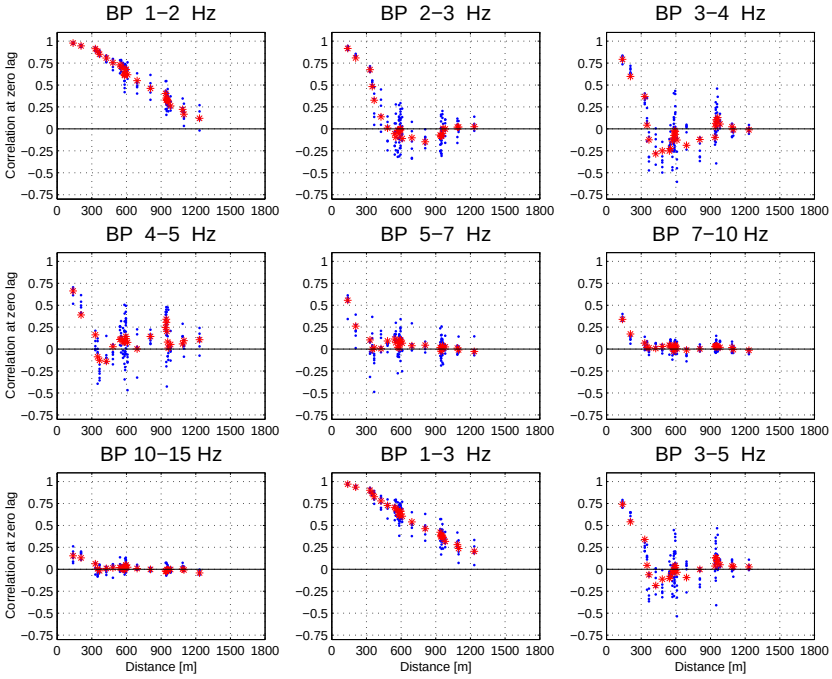

Figure 17: Median-value on top of all values for the cross-correlation for the **old** array at day time.

3.4 Summary of noise studies

Spectral studies confirm that the Hagfors array is located in a low-noise area. The intention to build an array with intra array spacings facilitating negative noise correlations was achieved. The new array has also the negative correlations for the longer intra array spacings that was missing for the old array. Unfortunately the shortest intra-array-spacings were lost with the new array configuration.

4 Signal studies

4.1 Signal correlation

The cross-correlation for both noise-data (blue dots) and signal-data (red for p-phase and green for s-phase) are shown in Figure 18. The noise cross-correlation is calculated for zero-lag and signal cross-correlation for best-lag (lag that gives correlation maximum). The figure shows that both phases are more or less separated from the noise-data for all frequencies.

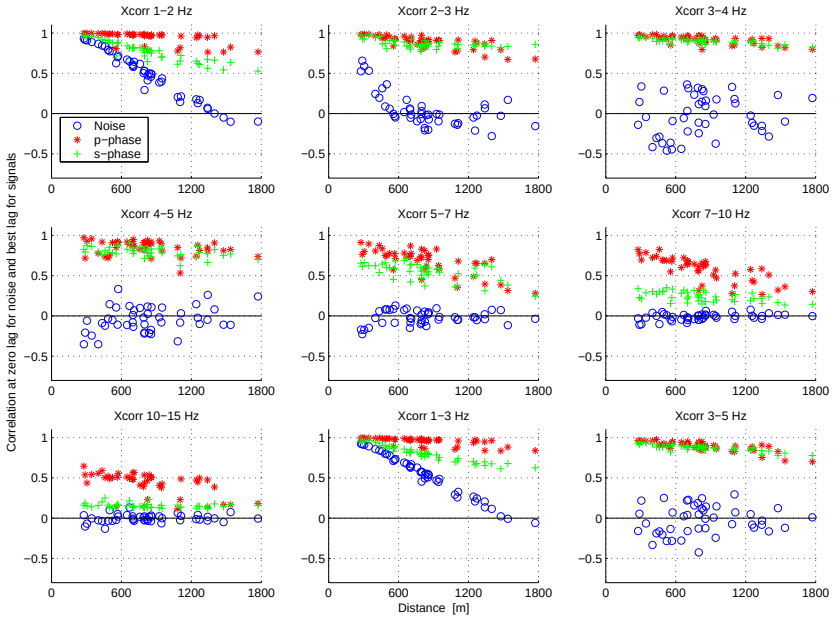

Figure 18: Cross-correlations for p- and s-waves of the Morocco earthquake in February 24, 2004 (red and green dots). The noise cross-correlations are displayed with blue dots.

Figure 19 shows the cross-correlations from two phases for a local explosion. The p- (red dots) and the s-phase (green dots) are well correlated in all frequency bands and can easily be separated from the noise.

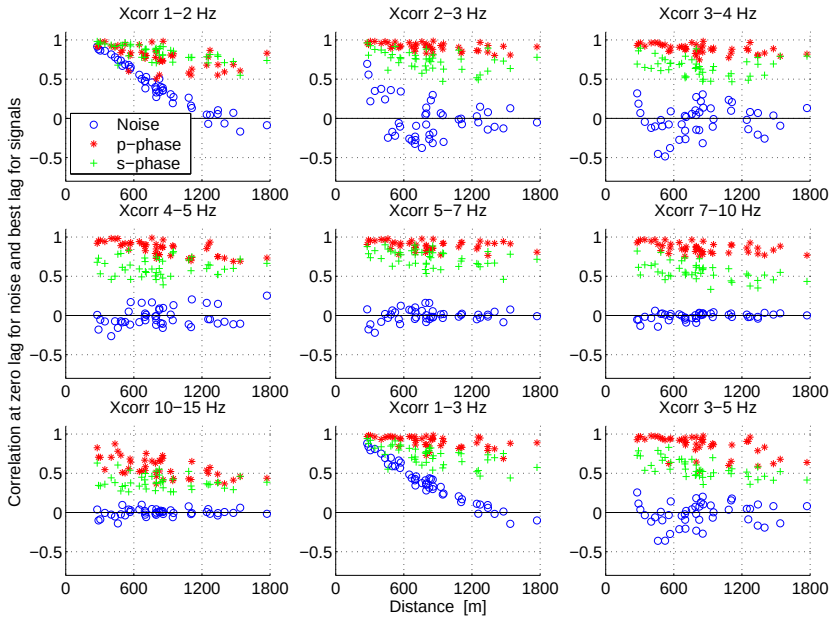

Figure 19: Cross-correlations for different waves from an explosion in Gävleborg in September 30, 2003. Noise cross-correlations from the time just before the event are displayed with blue dots.

4.2 Gain

When the cross-correlation for the noise and a signal is estimated the array-gain can be calculated from:

$$G^2 = \frac{\sum_{ij} S_{ij}}{\sum_{ij} N_{ij}}$$

where S_{ij} is the cross-correlation values, between channel i and j, for the signal (with best-lag) and N_{ij} for the noise (with zero-lag). For a perfectly correlated signal and uncorrelated noise this formula equals n, where n is the number of elements in the array. For the new array in Hagfors the best gain would be $\sqrt{10} \approx 3.16$ and for the old array $\sqrt{8} \approx 2.83$. Figures 20 - 22 shows array-gain for both new and old array for 3 events, one local (magnitude: 1.96), one regional (magnitude: 2.96) and one teleseismic event (magnitude: 6.2). The array-gain is normalized with $\sqrt{n}$. The array gain is lowest for the lower frequencies (1-3 Hz). That is due to the high correlation of the noise for the lower frequencies. Around 4 Hz the array gain has the highest values both for new and old array for all three of the events. If we look at Figures 14 or 15 the noise cross-correlation value is negative, for many intra-array spacings, in that frequency-band, that explains the high array gain around 4 Hz.

	Värmland 20030226			
	New Array		Old Array	
	Gain	dB	Gain	dB
BP 1-2 Hz	1.4204	3.0480	1.2994	2.2746
BP 2-3 Hz	3.8352	11.6758	2.6067	8.3218
BP 3-4 Hz	3.3306	10.4504	2.5915	8.2711
BP 4-5 Hz	3.7884	11.5692	2.0794	6.3587
BP 5-7 Hz	3.2512	10.2409	2.2588	7.0776
BP 7-10 Hz	2.9662	9.4440	2.2844	7.1755
BP 10-15 Hz	2.6506	8.4669	2.1395	6.6062
BP 1-3 Hz	1.4814	3.4135	1.3516	2.6172
BP 3-5 Hz	3.6816	11.3207	2.4310	7.7157
BP 1.5-4 Hz	2.3560	7.4434	1.9133	5.6357

Table 3: Gain comparison between new and old array

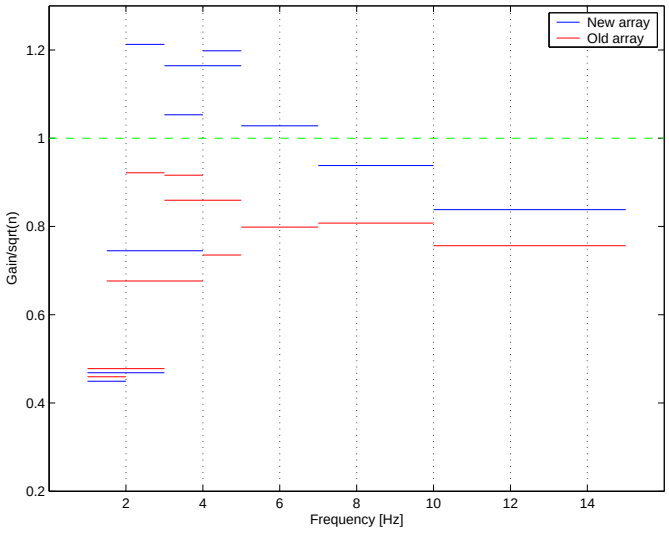

Figure 20: Gain values for the new (blue lines) and the old (red lines) arrays for February 26, 2003 local earthquake in Värmland. The array-gain is normalized with $\sqrt{n}$.

	Baltic area 20030228			
	New Array		Old Array	
	Gain	dB	Gain	dB
BP 1-2 Hz	1.2975	2.2622	1.1648	1.3248
BP 2-3 Hz	2.7822	8.8879	2.1118	6.4932
BP 3-4 Hz	2.9702	9.4556	2.2940	7.2117
BP 4-5 Hz	3.0396	9.6563	1.6398	4.2960
BP 5-7 Hz	2.4921	7.9315	1.7826	5.0212
BP 7-10 Hz	2.1896	6.8075	1.6801	4.5065
BP 10-15 Hz	1.9912	5.9824	1.7108	4.6639
BP 1-3 Hz	1.2652	2.0433	1.1731	1.3870
BP 3-5 Hz	2.8584	9.1225	1.8649	5.4131
BP 1.5-4 Hz	1.8087	5.1473	1.5357	3.7259

Table 4: Gain comparison between new and old array

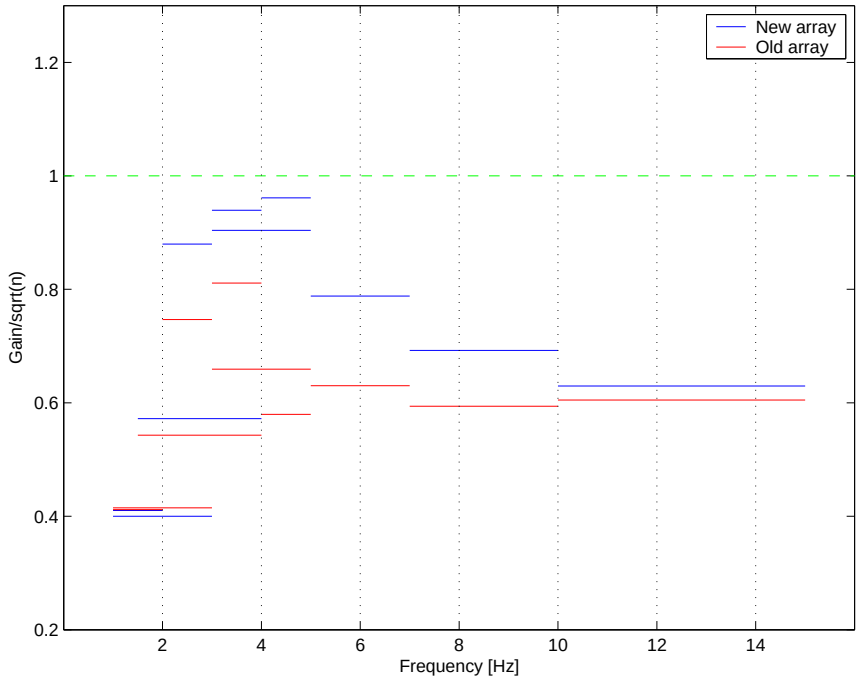

Figure 21: Gain values for the new (blue lines) and the old (red lines) arrays for February 28, 2003 regional event in the Baltic area.

	Indonesia 20030107			
	New Array		Old Array	
	Gain	dB	Gain	dB
BP 1-2 Hz	1.3101	2.3459	1.2208	1.7330
BP 2-3 Hz	2.8144	8.9878	2.1334	6.5815
BP 3-4 Hz	3.4969	10.8738	2.4436	7.7605
BP 4-5 Hz	3.5023	10.8872	1.6050	4.1095
BP 5-7 Hz	2.6241	8.3795	1.5803	3.9750
BP 7-10 Hz	2.4565	7.8063	1.7610	4.9152
BP 10-15 Hz	1.9240	5.6842	1.7122	4.6709
BP 1-3 Hz	1.2839	2.1708	1.2051	1.6207
BP 3-5 Hz	3.2733	10.2998	1.8090	5.1489
BP 1.5-4 Hz	1.7277	4.7495	1.4682	3.3359

Table 5: Gain comparison between new and old array

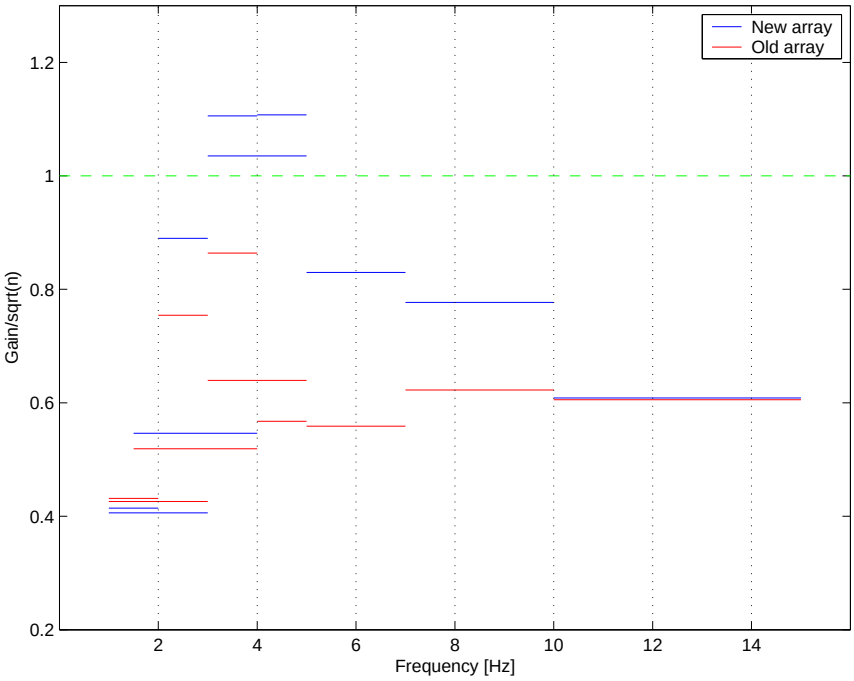

Figure 22: Gain values for the new (blue lines) and the old (red lines) arrays for January 7, 2003 teleseismic earthquake in Indonesia.

4.3 The Kazakhstan field experiment

On September 14, 2002, an underground explosion was carried out in eastern Kazakhstan, as part of an On-Site Inspection Field Experiment. The purpose was to simulate an illegal underground nuclear explosion.

It was a 12.5 ton chemical explosion detonated in a 200 meter deep borehole, drilled many years ago in preparation for a real underground nuclear explosion as part of the former Soviet Union's nuclear test program. Ground truth for the explosion was: September 14, 2002 at 06.31.04 UTC, Lat: 49.9069, Lon: 78.8172, Depth: 200 m. The distance from Hagfors Seismic Array Station to the test-site is 4130 km (37°) and the back-azimuth 76°.

On the unfiltered data is the signal from the test not visible but after filtering with a 2-4 Hz Butterworth bandpass filter can p-arrival be seen on both new and old array(see Figure 23).

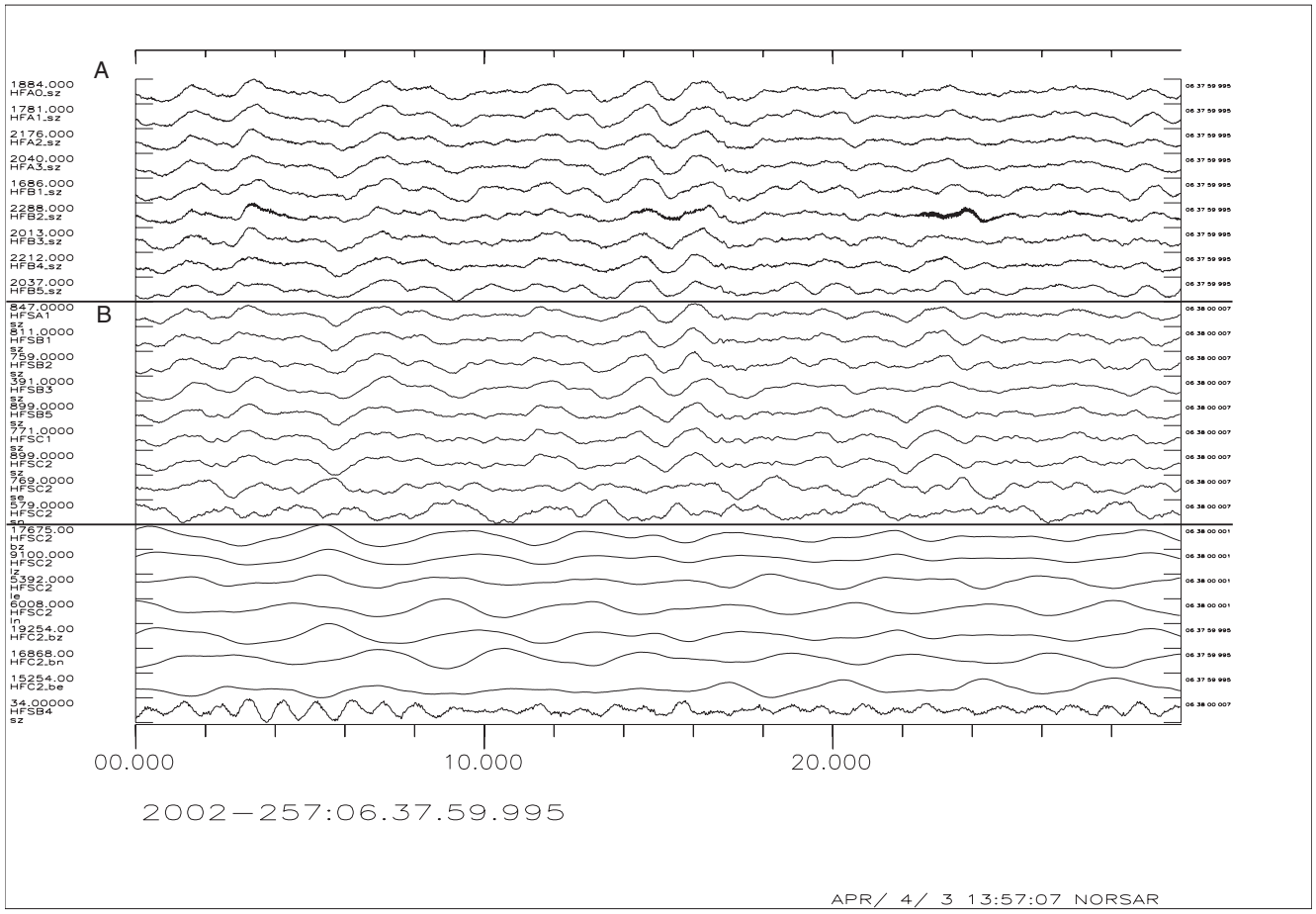

Figure 23: Unfiltered signals from the Kazakhstan field experiment. A is shortperiod-channels from the new array and B is shortperiod-channels from the old array.

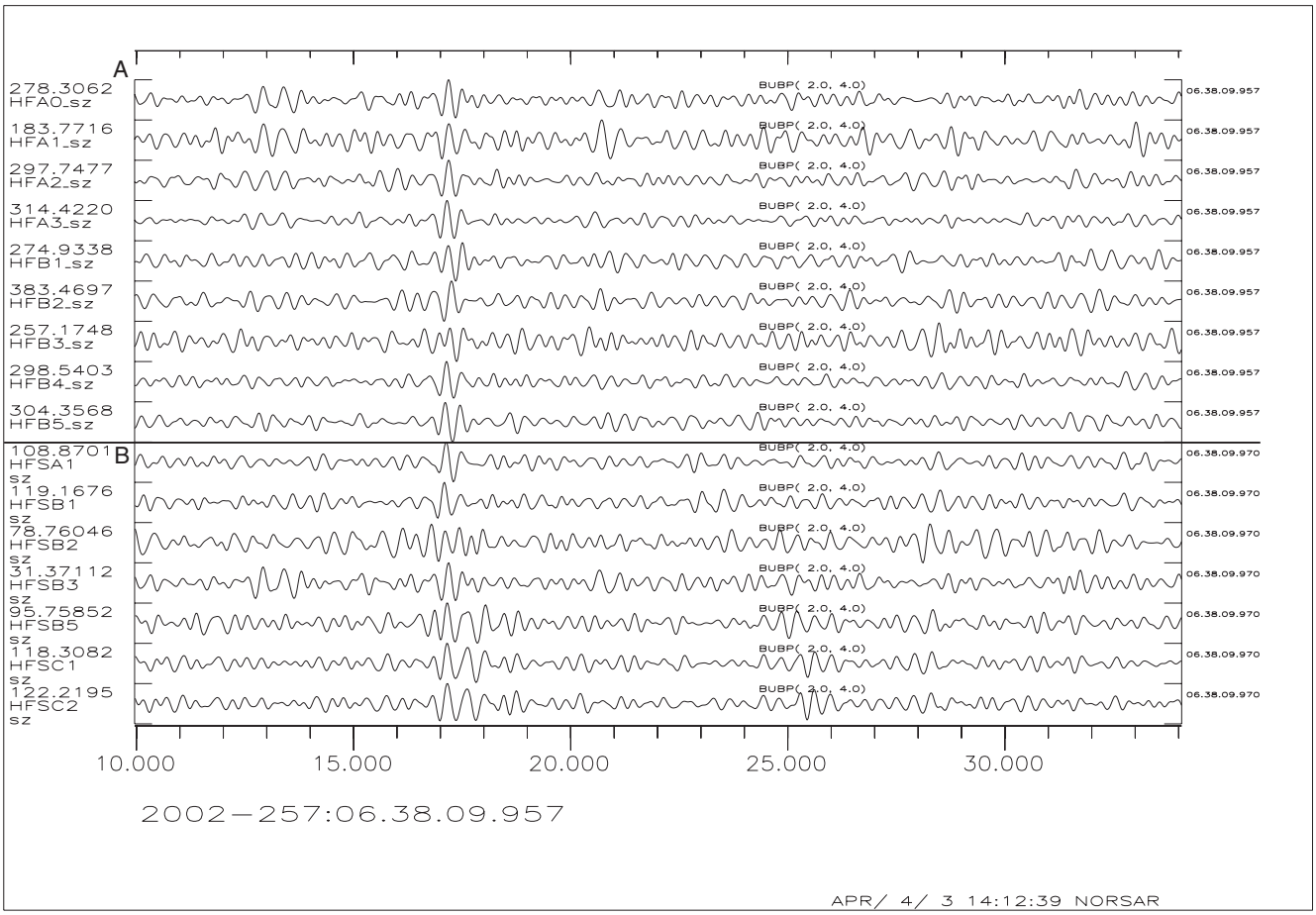

Figure 24: Filtered signals from the Kazakhstan field experiment. A is shortperiod-channels from the new array and B is shortperiod-channels from the old array.

On the p-wave beams the p-arrival is very clear. This indicates that Hagfors seismic array under favorable conditions is capable of detecting underground explosions down to 0.01 kT from this specific area.

4.4 Summary of signal studies

The array-gain is better for the new array, probably because of more elements in the array and longer intra-array-spacings. The correlations are also good for the signal data which gives improved array-gain. Frequencies around 4 Hz shows the best array-gain for the new array and 3-4 Hz for the old array. The new array has a good separation between signals and noise, even for teleseismic events. The Kazakhstan Field Experiment showed that the new array has very good detectability from this specific area.

5 Event analysis at Hagfors

The following sections evaluate and, where possible, compare, the event detection capabilities of the two arrays in Hagfors. This evaluation is based on processing of the Hagfors arrays both at the International Data Center (IDC) of the CTBTO in Vienna, and at NORSAR, Norway. The result of the processing is compared with different bulletins, such as the CTBTO Reviewed Event Bulletin (REB), the NORSAR regional reviewed bulletin and the Swedish National Seismic Network (SNSN) bulletin.

We note again that the upgraded Hagfors array was operational, including preamplifiers, on April 5, 2002; that the old and new systems ran in parallel between April 5, 2002 and September 21, 2003; and that the new array was certified at the IMS on December 17, 2002.

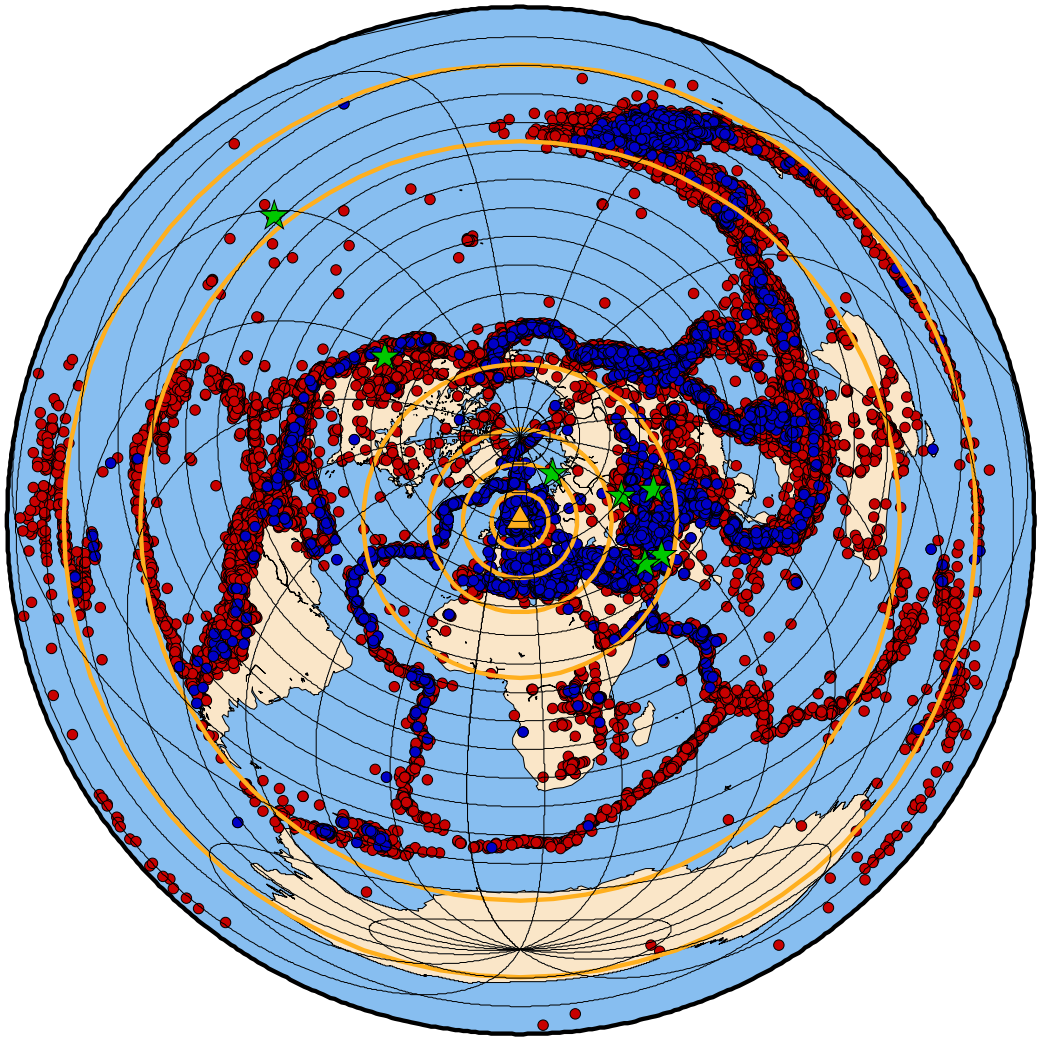

Figure 25: Map showing REB events between 1/1-2000 and 12/10-2003. All registered events in red, those with Hagfors contributions in blue. The orange circles indicate distances of 0°-10°, 10°-20°, 20°-32°, 32°-55° and 133°-160° midpoint angle intervals from Hagfors.

5.1 IDC processing and the REB

The Hagfors array is an Auxiliary Seismic Station in the International Monitoring System (IMS) network and as such does not normally have a continuous data feed to the IDC. The IDC requests data from Hagfors for certain events and then uses that data to better constrain the event definition parameters and increase accuracy. The IDC routines for when to include Hagfors data are not completely clear to us, they are based on the distance from the

station to the event, but also seem to take into account regions of the world from which there are well defined phases at Hagfors, see figure 25.

This study comprises REB:s from January 1, 2000 to October 12, 2003, and aims at a broad view of Hagfors's contribution to the REB during these years. Also, since the upgraded Hagfors array was switched into the IDC processing on December 17, 2002, we will be able to observe how that changed the accuracy and significance of the Hagfors data.

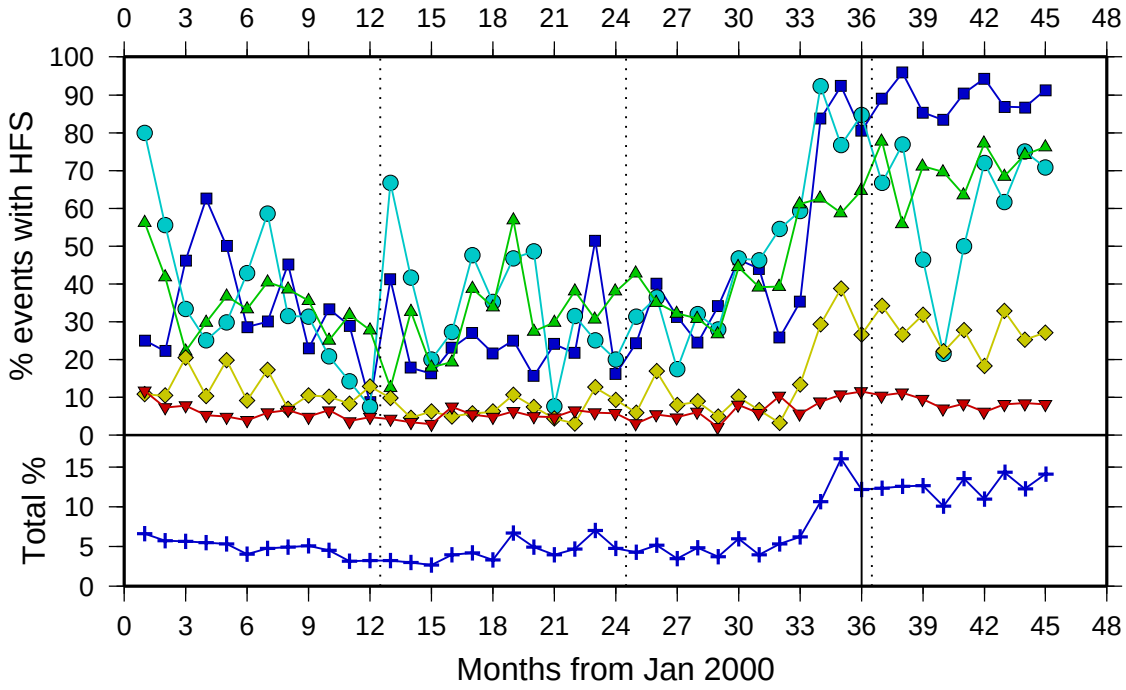

Figure 26: Upper: Percentage of REB events that Hagfors contributed to for different distances from the array. Dark blue squares: 0° - 10°; Light blue circles: 10° - 20°; Green triangles: 20° - 32°; Yellow diamonds: 32° - 55°; Red inverted triangles: 133° - 160°. The solid line denotes the switch to the upgraded HFS array, the dotted lines are new years. Lower: Percentage of total number of events in the REB that Hagfors contributed to.

5.1.1 Hagfors data in the REB

During the studied time period the REB contains 81972 events. Data from Hagfors was used for 5855 events, see Fig. 25, concentrated in certain regions of the world. We see from Fig. 25 that Hagfors data is mainly utilized for events in Europe and the mid-east, but that there is also a significant contribution to events located in central Asia and as far away as the Tonga trench (PKP and related core phases).

If we subdivide the REB data based on the events' distances from Hagfors, see Fig. 26, we observe that Hagfors is present on more of the closer events compared to the distant events, as expected. More importantly, however, we see that there is a significant shift in the level of the curves from approximately month 33, i.e. October 2002. This shift is not due to the incorporation of the upgraded Hagfors array into the IDC processing, since that did not occur until December 17, 2002. Contacts with the IDC staff confirmed that on September 24, 2002, a new version of the auxiliary station request software was put into operation. The new version requests data from all auxiliary stations within 30° of the event, which explains the sharp rise in the closer curves in Fig. 26. It does, however, not explain why there are more requests for the 32° - 55° events. We see from Fig. 26 that the change utilizes Hagfors in a more consistent way, and also that the change has brought about a significant increase of Hagfors data in the IDC processing.

As this report does not aim at seismicity studies of specific regions of the world, we have not investigated how the REB compares to other world-wide seismic bulletins. We have for reference included the period's REB events in the regions of the central Asian nuclear weapons test sites, Iran/Iraq and the Korean peninsula, see Appendix B. There we plot all events in the REB as well as the events with Hagfors contribution.

5.1.2 Azimuth and slowness residuals

We have compared the azimuth and slowness residuals as calculated by the IDC for the Hagfors array for four different areas at different distances and azimuths and where there is sufficient Hagfors data in the REB. The residuals are calculated as observed minus theoretical values.

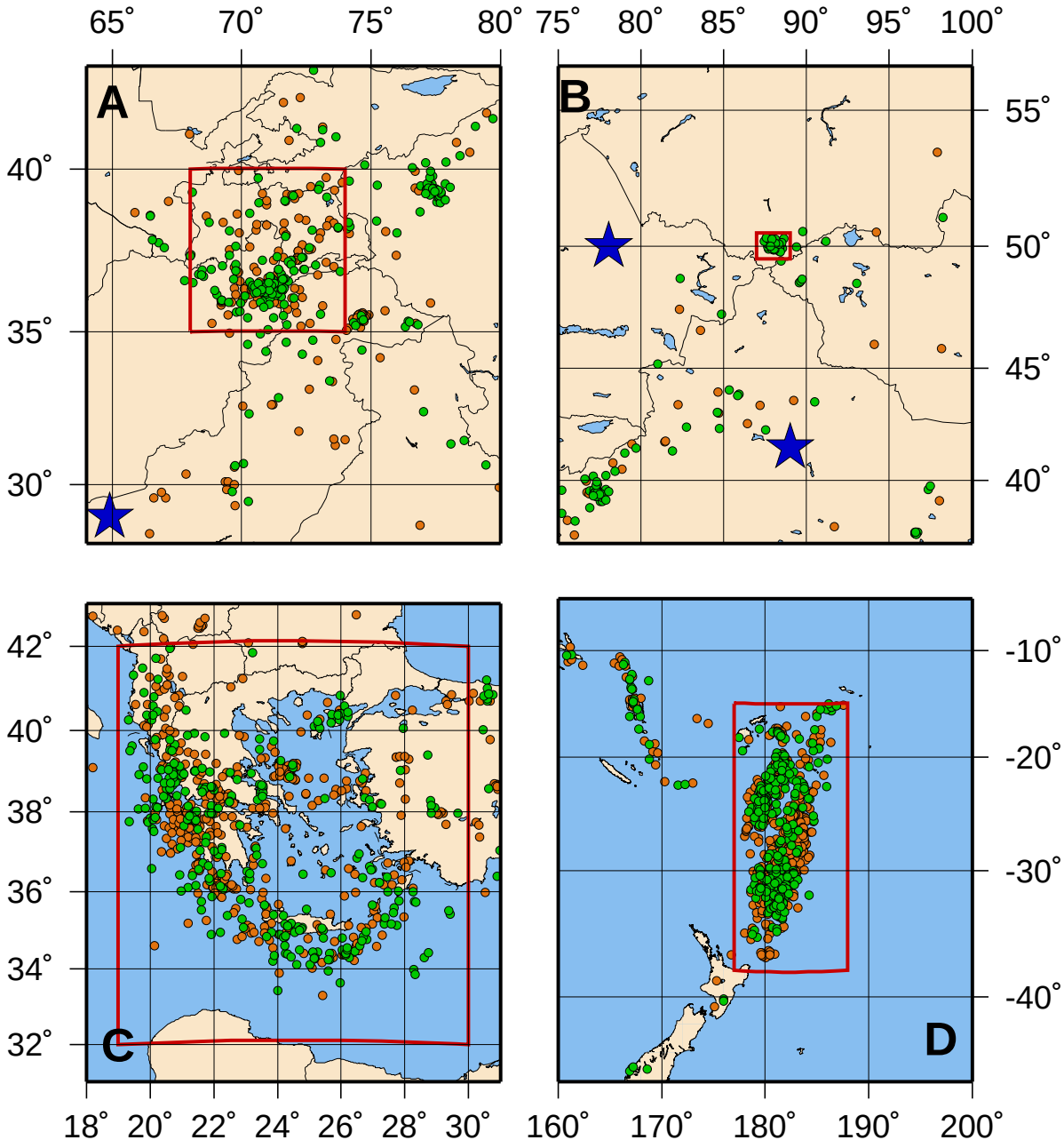

Figure 27: Maps showing the regions, red boxes, from which we studied azimuth and slowness residuals. The blue stars are nuclear weapons test sites. A) Northern Afghanistan B) Russia-Mongolia border C) Greece D) Tonga-Kermadec trench

Northern Afghanistan We used 254 events occurring all through the studied time period from the area of northern Afghanistan, northern Pakistan and Tajikistan, see map A in Fig. 27. These events have a back-azimuth of approximately 98° and a slowness of approximately 10 s/deg for the first arriving P-phase. The smallest events with HFS contribution from the area are of magnitude $m_b = 3.1$, the median for the group is 3.8.

Figure 28 shows the distribution of azimuth and slowness residuals with time. For clarity of presentation, time is here represented by the event number and the events are numbered in chronological order. We see clearly how the slowness residuals change character as the upgraded HFS array is entered into the IDC processing. Using the old array the slowness residuals show evidence of a bimodal distribution, with one mode very close to the model slowness value and the other significantly higher than the model slowness. With the new array, this bimodal shaped distribution disappears and is shifted to +2.3 s/deg, i.e. larger slowness than the model predicts. The standard deviation is significantly decreased with the new array, but the median is 2.0 s/deg further from the model slowness. The azimuth residuals show a less dramatic change, but we see that there is an almost four degree shift in the median and that the standard deviation reduces as the new array enters the processing. This behavior of the residuals do not change if we concentrate on the core group of events in Fig. 27A and is thus not a small scale location effect.

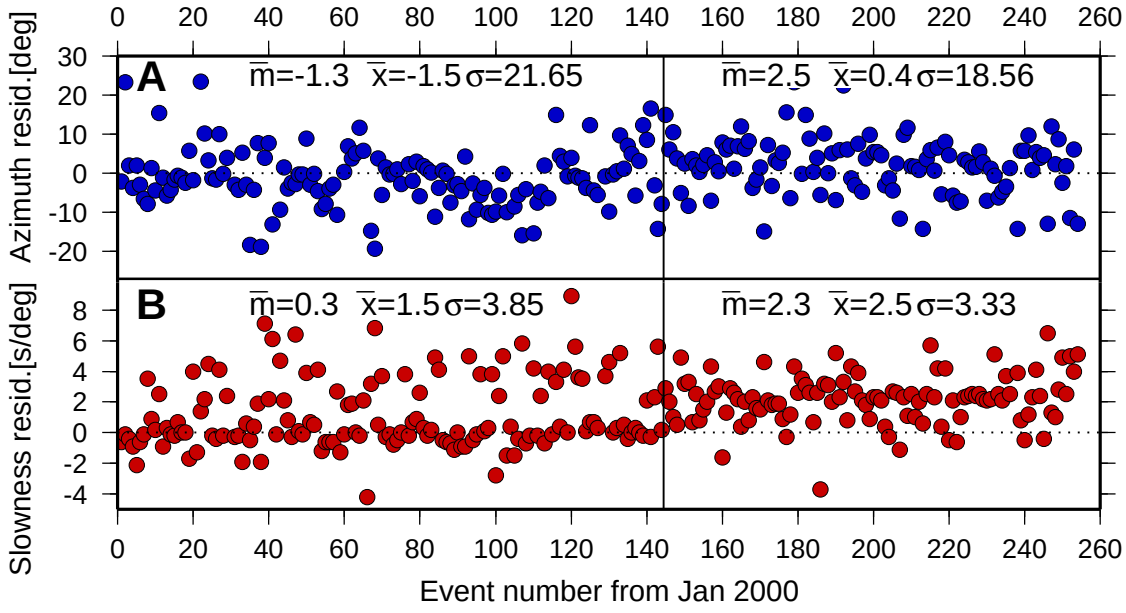

Figure 28: A) Azimuth and B) slowness residuals for 254 events from the northern Afghanistan area. The solid vertical line denotes the change over from the old to the new array in the IDC processing. $\bar{m}$ is the median, $\bar{x}$ the mean and σ the standard deviation of the residuals.

Russia-Mongolia border We studied a small group of 85 events on the Russia-Mongolia border, see Fig. 27B. These events took place in the two weeks of 27/9-03 to 12/10-03 and therefore occurred solely during the operation of the upgraded HFS-array. Back azimuth for the events are 81° and P slowness approximately 9 s/deg. The minimum magnitude in the group is $m_b = 3.7$, the median 4.0.

In Fig. 29 we have plotted azimuth and slowness residuals for the events. We see that azimuths are not very well estimated for these events, the median residual is +11.2° and the standard deviation 28°. The slowness residuals cluster around the model value, the median is 0.8 s/deg., but have a rather large standard deviation, 5.4 s/deg. It is interesting to compare these results with the northern Afghanistan group above. Both event groups are almost equally far from Hagfors, 43° for northern Afghanistan, 41° for this group, but the azimuth and slowness residuals are significantly larger for this group. The residuals could be due to poorer signal-to-noise ratios for this group, which has a median SNR of 5.5 compared to the northern Afghanistan group's median SNR of 9.5.

Greece In order to study azimuth and slowness residuals on closer events we chose the REB registered events from Greece, 710 events with HFS contribution. These events were registered during the entire studied time period, have a back-azimuth of approximately 158°, the distance is approximately 25° and they have a P slowness of approximately 11 s/deg. The minimum magnitude is $m_b = 3.0$, the median 3.9.

We see again in Fig. 30 that the residuals are more concentrated when the new array enters the processing. Azimuth residual standard deviation drops from 20° to 11° and in slowness the standard deviation decreases

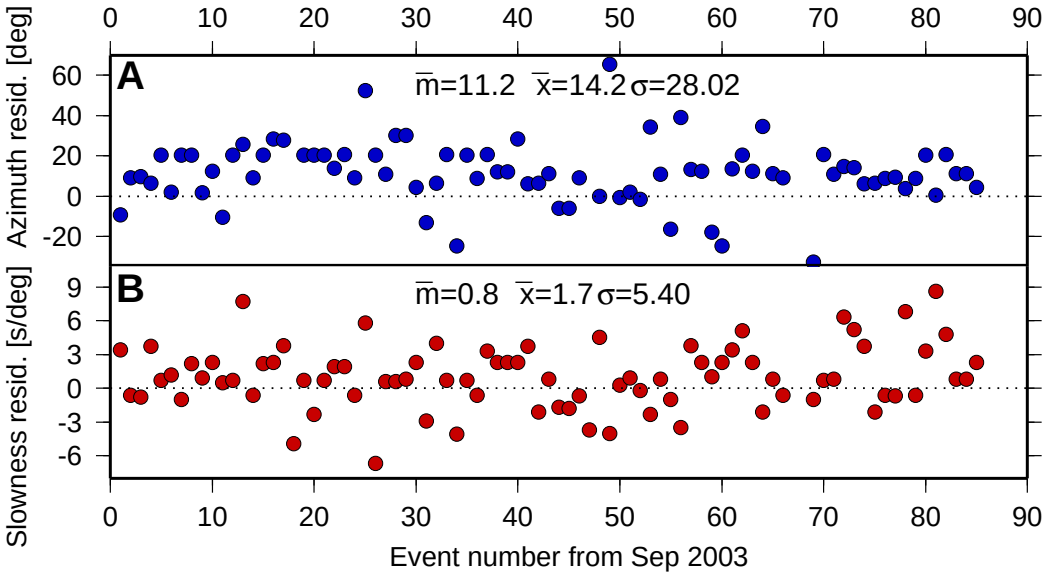

Figure 29: A) Azimuth and B) slowness residuals for 85 events from the Russian-Mongolian border area. The solid vertical line denotes the change over from the old to the new array in the IDC processing. $\bar{m}$ is the median, $\bar{x}$ the mean and σ the standard deviation of the residuals.

from 3.38 s/deg. to 2.56 s/deg. There is a slight decrease in the median azimuth residual when the new array comes in so that the new array underestimates azimuths by approximately 2.3°. The slowness estimate is, conversely, slightly overestimated, by 1.2 s/deg. Compared to the two groups of events above, the Greek events show smaller residuals and less deviation, as expected from closer events.

The Greek events are spread over a fairly large region and it is possible that there is some structure in the residuals with respect to where the events are located. We have, however, not looked into that issue.

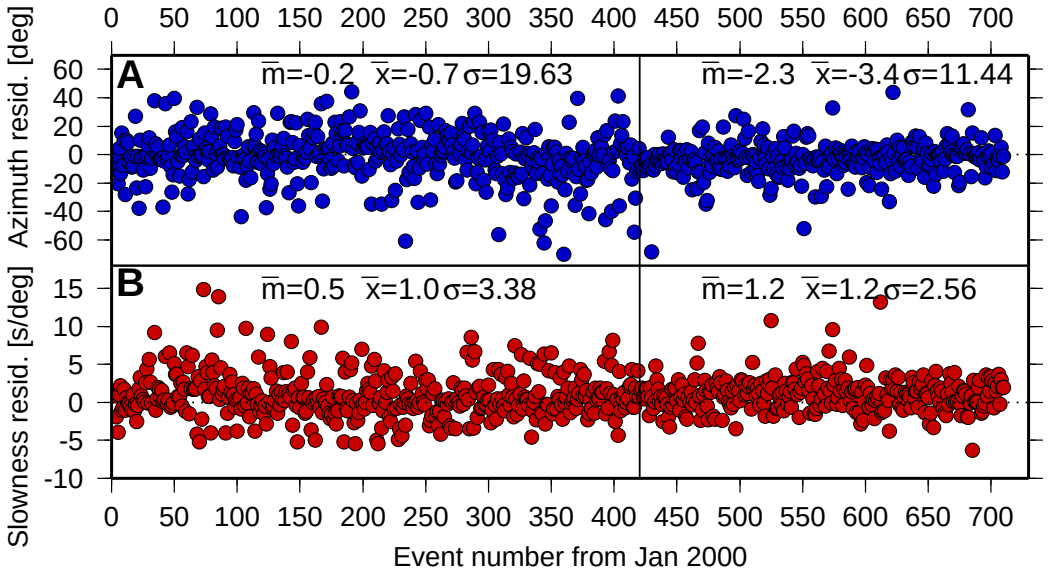

Figure 30: A) Azimuth and B) slowness residuals for 710 events from the Greece area. The solid vertical line denotes the change over from the old to the new array in the IDC processing. $\bar{m}$ is the median, $\bar{x}$ the mean and σ the standard deviation of the residuals.

Tonga-Kermadec trench The Hagfors contribution to the Tonga-Kermadec trench events is a result of the IDC policy of using stations where specific phases show specifically well. Hagfors is ideally situated to record the PKP (and associated core phases, PKPbc, SKPbc, PKhKP) from Tonga. The group contains 732 events, they have a back-azimuth of approximately 67°, distance is approximately 143° and PKP slowness 3.3 s/deg.

The PKP phase comes in close to vertically beneath the Hagfors array, making azimuth estimation rather difficult. This is clearly shown in Fig. 31 where the azimuth residuals have a standard deviation of 67° with the old array and 58° with the new array. We also see that there is a large difference in the median azimuth between the old and new arrays, where the new array overestimates azimuth by 41.5° compared to the old array's 19° overestimation. The slowness residuals, conversely, are rather well estimated and with a surprising increase in standard deviation of the residual with the new array.

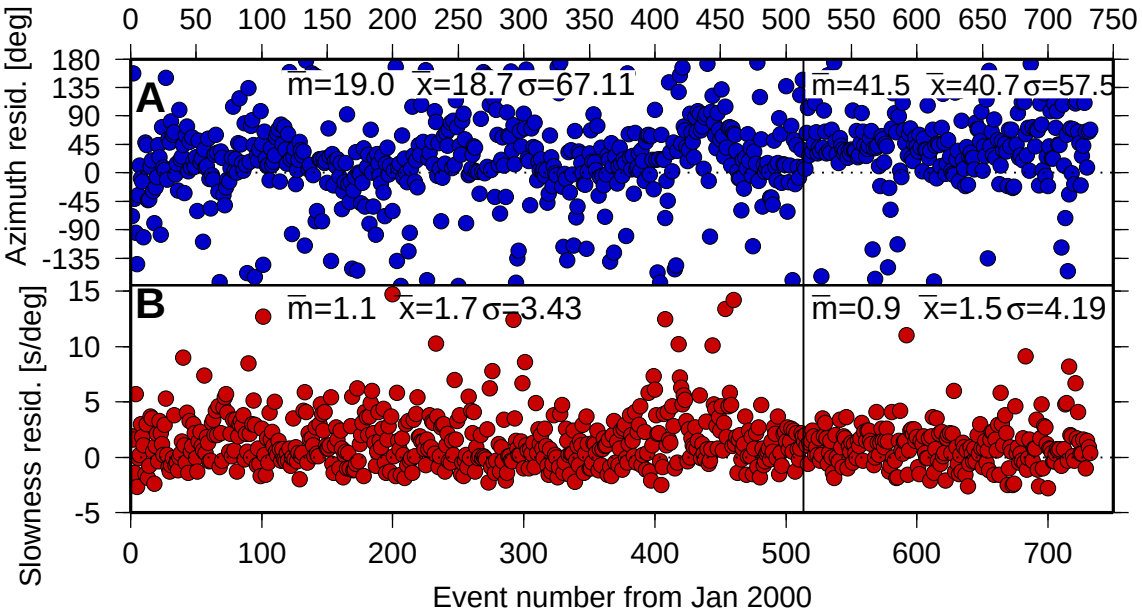

Figure 31: A) Azimuth and B) slowness residuals for 732 events from the Tonga-Kermadec subduction zone. The solid vertical line denotes the change over from the old to the new array in the IDC processing. $\bar{m}$ is the median, $\bar{x}$ the mean and σ the standard deviation of the residuals.

5.1.3 Summary

Since the upgrade of the IDC auxiliary seismic station request software in September, 2002, Hagfors data is incorporated in the IDC processing of all events within a 30° radius of the station. Not all of these events are detected at the Hagfors array, but towards the end of 2003 Hagfors contributed to approximately 77% of them. There is also a significant Hagfors contribution to events in central Asia and, with the PKP related phase, to the Tonga-Kermadec seismicity. As pointed out in the beginning of this section, and clearly expressed by the results, Hagfors contributions to the REB is only to a minor degree the result of the array's qualities and more an issue of IDC policies.

Our study of four regions of the world shows that with the new Hagfors array uncertainties in azimuth and slowness determinations are generally improved, compared to the old array. It is interesting to note, however, that the medians of azimuth and slowness residuals with the new array show larger deviations from the correct/model values than the old array residuals. This difference in the behavior of the residuals is not due to a major change in the azimuthal response of the array after the upgrade. As was shown in sections 2.2 and 2.4, the azimuthal variation in array response is very similar at the two arrays, although the resolution of the new array is significantly better than the old. The tendency toward better resolved, yet less accurate residuals should be further investigated and will facilitate the implementation of phase/azimuth/region dependent array corrections.

5.2 EP processing at NORSAR

The Hagfors seismic array data is processed at NORSAR, Norway, for phase detection (DP) and event detection (EP). This is a a regional event detection algorithm which focuses on Scandinavia, from northern Germany in the south to Svalbard in the north. It is an entirely automatic process, which during the studied time period was not optimized for the new array. During the time of simultaneous operation of the old and new seismic arrays at Hagfors, 2/4-2002 to 21/9-2003, DP and EP processing was carried out on both of the arrays. Here, we will report some statistics of the operation of the arrays and compare the performance of the two. During the studied period, data is missing between 22/6 - 8/7 2002.

The EP algorithms define an event ([5] and Schweitzer, personal communication) based on the identification of P and S phases with similar azimuths. If there are P and S phases with similar azimuths within a certain time window, the process tries to define an event which would produce phases with the observed time differences at the array. Phase identification is performed by f-k analysis and phase-slowness relationships. There is no overall quality measure produced by the EP processing, events are defined if they pass internal residual limits. These residual limits are unique for individual arrays and need tuning, which has currently not been performed for the new array at Hagfors.

The old and new arrays are distinguished below by the use of the abbreviation HFS for the old array and SVE for the new array.

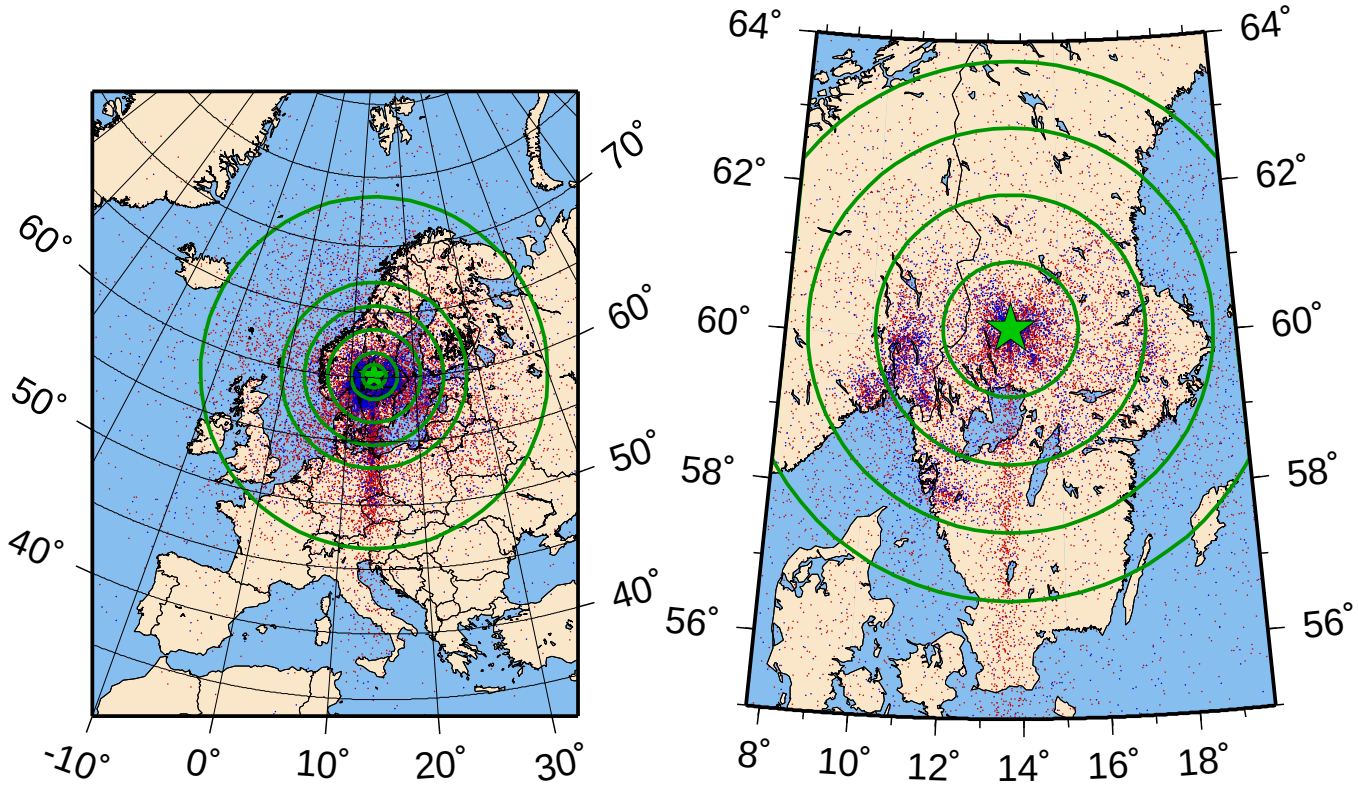

Figure 32: Distribution of events defined in the EP-processing for the new array SVE, red, and the old HFS, blue. The location of Hagfors is marked with a green star. In the map of Europe, to the left, circles are drawn in green at distances of 100, 200, 400, 600, 800 and 1500 km from Hagfors. In the map of southern Sweden, right, the circles are at 100, 200, 300 and 400 km.

5.2.1 EP statistics

During the studied time period the old HFS array defined 8081 events and the new array, SVE, defined 21221 events, see Fig. 32. Most of these events are probably spurious associations of phases but we will refer to them as events for the remainder of this section. In spite of the probably large amount of erroneous associations, it is interesting to note the factor of 2.5 increase in detections at the new array. Before examining the event locations

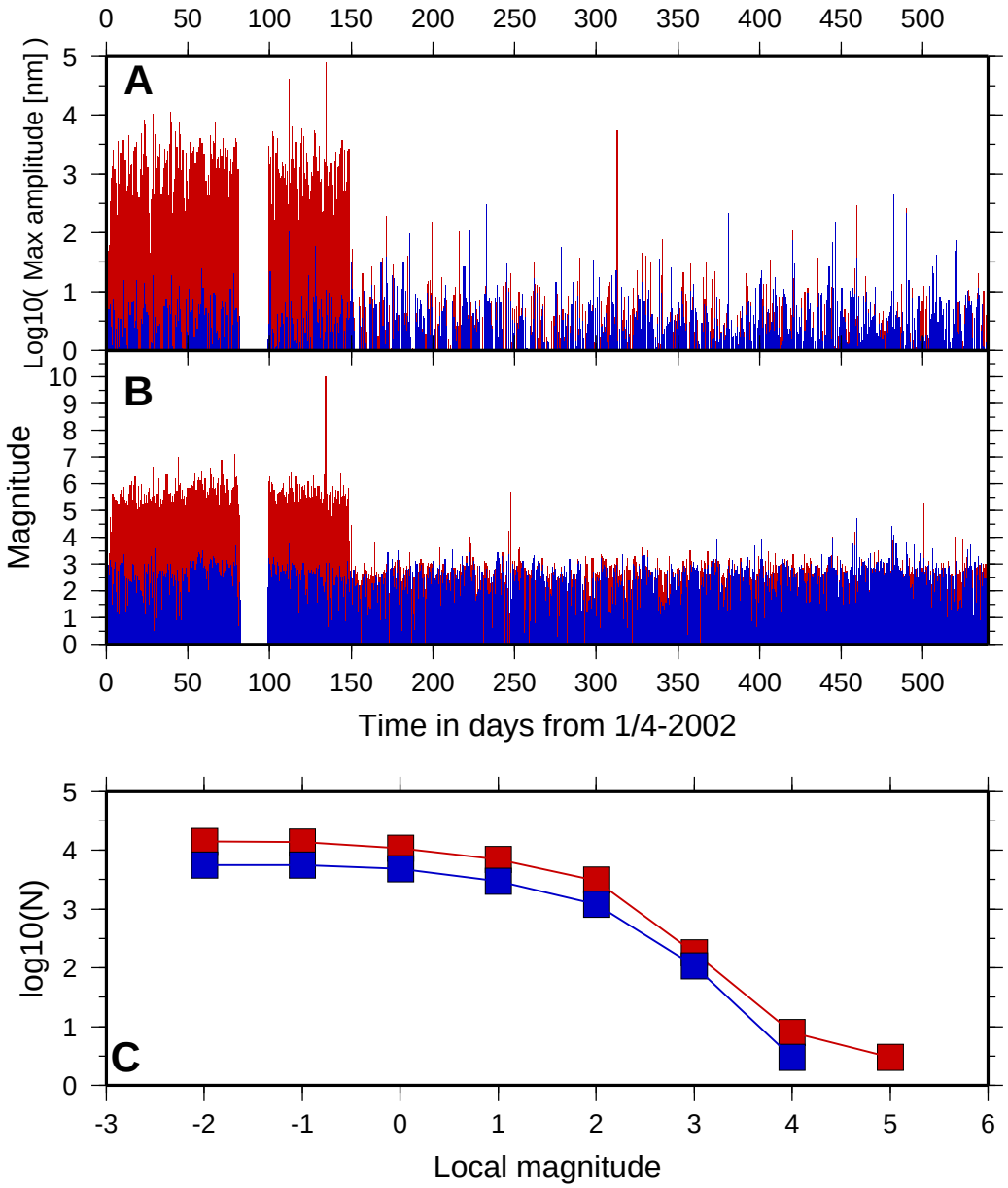

Figure 33: A) Logarithm of the maximum amplitude of the event defining S-wave, in nm, vs time in days from 1/4-2002. Red, SVE array, blue, HFS array. B) Local magnitude estimated for all events vs. time in days from 1/4-2002. Colors as above. C) Gutenberg-Richter plot of number of events above a certain magnitude vs. magnitude. Here we only use events after day 148, i.e. 27/8-2002. Colors as above.

we note that there was in the beginning of the time period, from 2/4-2002 to 27/8-2002, a problem with the magnitudes at the new array, see Fig. 33. Magnitudes are estimated from the amplitudes of S/LG phases and we see that the amplitudes were erroneously calculated before August 28, which affected the magnitude estimates. We note in Fig. 33C, which only uses data after 27/8-2002, that even after correction of the amplitude calculation, the SVE array estimates slightly higher magnitudes than the HFS array. We also note that there is a clear deficiency in small magnitude events at the arrays. Fig. 33C gives the impression that the completeness level of the arrays is as high as magnitude 2.

Although rather cluttered, one feature stands out in Fig. 32. It is the southbound line of events from Hagfors, extending all the way into northern Italy. In order to investigate the spatial distribution of events we plotted azimuth and distance from Hagfors distributions for the two arrays, see Fig. 34. We immediately note in Fig. 32A

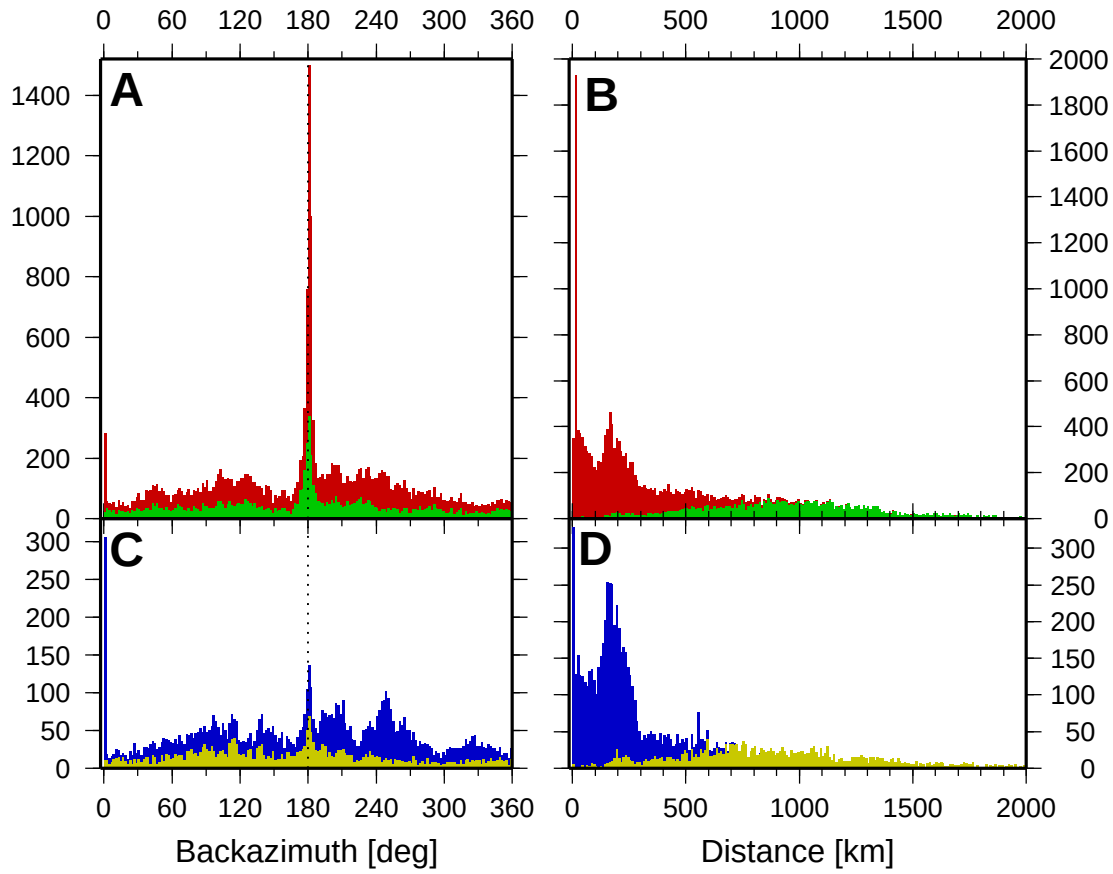

Figure 34: A) Azimuth distribution of detected events at the SVE array. Red are all events, green are events with magnitude larger than 1.25 (see text for more details). B) Distance from Hagfors distribution for the SVE events. C) and D) show the same information for the HFS array, with blue being all events and yellow all events above magnitude 1.5.

the large number of events at SVE due south of Hagfors. These "southern" events are also present at HFS but in much smaller numbers, also relative to the total number of events. It is interesting to note that there is a peak due north of Hagfors as well, about 300 events high at SVE and equally high at HFS, thereby dominating the HFS azimuth distribution. If we concentrate on the larger events (M >= 1.5 at HFS and M >= 4.9 for the first 148 days at SVE, then M >= 1.25. We use a lower threshold at SVE in order to create data sets that are equally large relative to the total number of events at the two arrays.), the green and yellow histograms in Fig. 34, we see that the southern peak still dominates the histograms, but that the northern peak seems to have vanished.

Looking at the distance histograms in Fig. 34B and D, we see that there is a large number of very close events. Interestingly, these events are in the second 10 km bin at SVE but in the first at HFS. There is a small trough in the distribution around 100 km, at both arrays, and then a second maximum around approximately 180 km. We see from Fig. 32 that the 180 km maximum is related to events located in the Oslo region. Event numbers fall off rapidly to about 300 km and then there is a more gradual decrease out to 1400-1500 km, after which the activity is very low. At the HFS array, we see that at approximately 750 km the yellow distribution completely covers the blue distribution, indicating that at larger distances there are no events smaller than magnitude 1.5. The situation is a little different at SVE, where there is a more gradual increase of the green, large events, distribution. It is not until approximately 1100 km that there are no smaller events than magnitude 1.25, which is a little surprising. This feature of the distribution could, however, be influenced by the difficulty of homogenizing the SVE data sets before and after August 28, 2002.

We have, as of yet, not fully investigated the many events defined due south of Hagfors. Studying the temporal distribution of events we observed that the 180° events persist all through the studied time period. It is likely that the events are due to a nearby cultural noise source, the obvious candidate being the Hagfors steel works, located approximately 15 km due south of the arrays. Further investigations of these events are underway.

Signal-to-noise ratios and event quality As noted above, it is somewhat difficult to assess which events are real and which are just spurious associations of phases without actually going through the waveform data. The EP-processing does not produce an overall event quality measure, we are left with only the signal-to-noise ratios

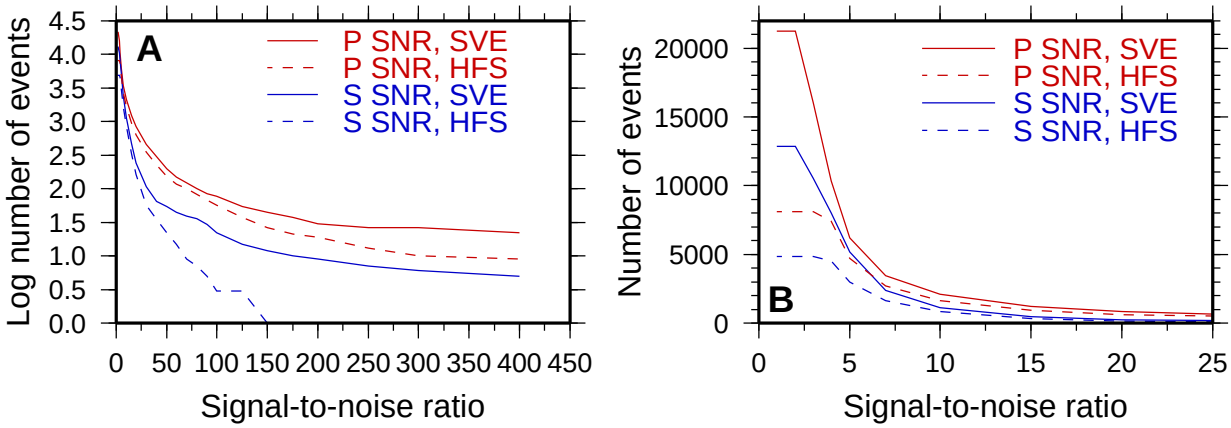

Figure 35: A) Logarithm of the number of events vs. signal-to-noise ratio. Red lines are P-wave SNR:s, blue lines are S-wave SNR:s, full lines are from the SVE array, dashed lines from HFS. B) Detail of the first part of A.

(SNR) available for the individual phase detections. Therefore, to compare the SVE and HFS arrays in terms of how many real events they detect and locate is not a very straightforward issue. We made an attempt by looking at the SNR:s for the P- and S-waves used to define an event, see Fig. 35. SNR is calculated as a simple ratio of the detectors short-term to long-term averages, SNR = STA/LTA. In the SVE processing, there are 26 events where the P-wave has an SNR above 300, in the HFS processing there are 10 such events. Only five of these events are common to both arrays, and the remaining five events on HFS cannot be found on SVE even if the SNR is lowered to 10. Although we have not checked the waveform data, these five "undetected" events are probably just spurious phase associations. Of the five common events, four can be found in NORSAR's regional reviewed bulletin and are, thus, proper events. The remaining event has very similar location, in the Värmland region, on both arrays and a magnitude around 1 so it is probably a proper event but too small to enter NORSAR's bulletin.

We see that high SNR, by itself, is not a good measure of the likelihood of an EP entry being a "real" event. This is, of course, not surprising seeing that a nearby noise source might very well produce a high amplitude transient, which might then be associated with lower amplitude, unrelated, noise to an event. Even for proper events the EP algorithms do not always choose the correct phases in the event association process. We list some issues with the EP-processing that we have encountered in Appendix C.

5.2.2 Comparison with the NORSAR regional reviewed bulletin

NORSAR, the Norwegian NDC, publishes an analyst reviewed, regional event bulletin (NRRB) for the Nordic countries. The Hagfors seismic array data is used in the production of the bulletin and we have chosen this bulletin as "ground truth" for our evaluation and comparison of the two arrays at Hagfors. The use of the NRRB may bias the results present below somewhat since data from the old HFS array was used in the production of the NRRB all through the time period we study here. We will compare the bulletin with the results of single array processing, using the EP-algorithms, at the two arrays.

For each event in the NRRB we will search for an event defined by the EP-processing where at least one P, or one S, wave phase fit the estimated arrival time at Hagfors for that phase. Note however, that we do not search for individual phase detections fitting the estimated arrival times, we search for an event that the EP-processing has defined. For the travel-time calculations we have used NORSAR's velocity model for Scandinavia [5] and the TauP program [6].

During the time of simultaneous operation of the two arrays, 1327 events were reported in the NORSAR bulletin. The magnitude of the events range from local magnitude 1.4 to 5.1, with most events above magnitude 2. Hagfors (i.e. HFS) phases were used for location of 857 of the events, according to the bulletin. Searching through the EP single array processing, we found that 454 of the events had event definitions at HFS and 464 had definitions at SVE, see Fig. 36. The EP-processing, thus, detects only approximately half of the events that the NORSAR

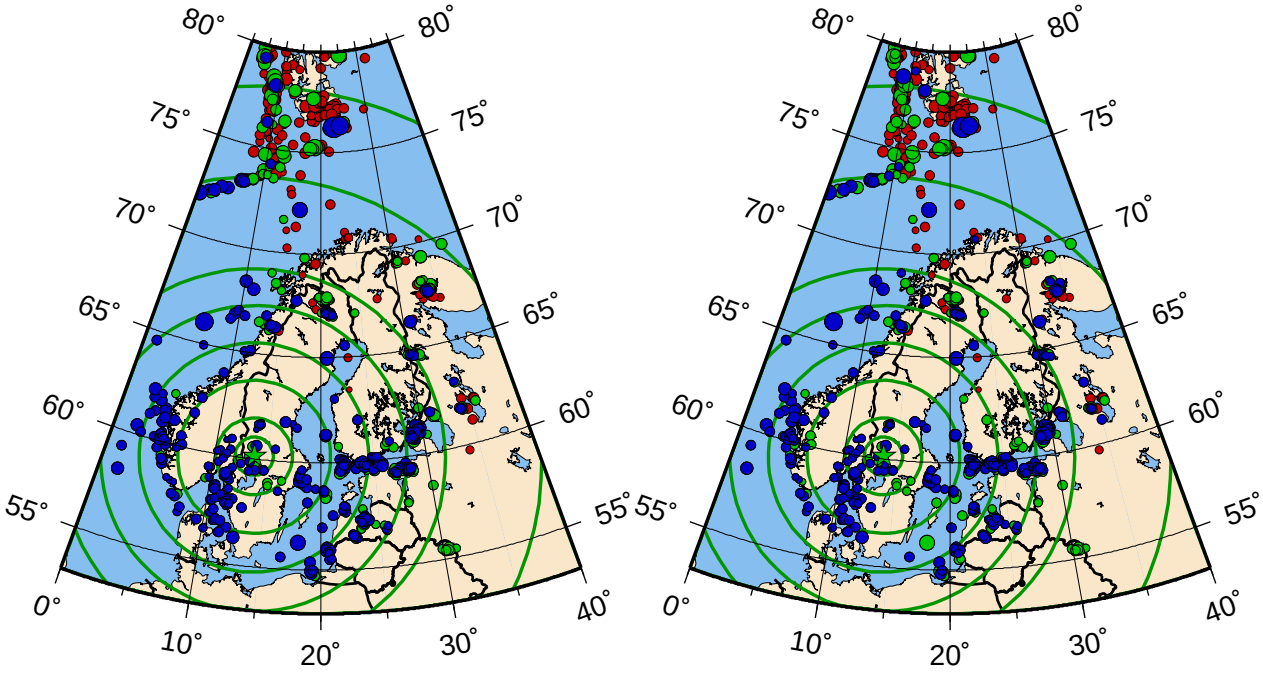

Figure 36: The red dots show the distribution of events in the NORSAR regional reviewed bulletin for the time period 2/4-2002 to 21/9-2003. Green dots overlay the red for events for which there are Hagfors readings in the bulletin. The size of the circles are proportional to event magnitudes. Hagfors is marked with a green star, green circles show distances of 100, 200, 400, 600, 800, 1000, 1500 and 2000 km from Hagfors. Left) Events identified by the HFS array, in blue, overlay the green/red dots. Right) Events identified at the SVE array, in blue, overlay the green/red dots.

operator is able to pick out, with the aid of data from the other Nordic seismic arrays.

In Fig. 36 the events in the NRRB have been plotted as red circles. These red circles have then been overprinted with other colors for events that also belong to other groups, such as being defined at one of the arrays. This convention of overprinting events in the figures is adhered to all through the entire section. We see in Fig. 36 that the two arrays pick up approximately the same events (blue dots), covering western Norway and the Swedish west coast very well.

The events in eastern Sweden, southern Finland and the Baltic countries are also well resolved, with some peculiar failures in south central Sweden and in the Värmland region (the latter are difficult to see due to the small scale of the maps). The mining activity in Gällivare is well identified but not that in Kiruna, an additional 100 km to the north. Most of the events within a 1000 km radius from Hagfors have Hagfors contributions in the NRRB (green dots), so there are clear phase detections at the arrays but the EP algorithms have not always succeeded in associating the phases to an event (blue dots). There are three obvious clusters of this type of events, where the NRRB has Hagfors detections but the EP-processing fails, one in Kiruna, one in southern Finland close to Helsinki and one on the border of Belarus and Russia, just outside the 1000 km radius. Beyond 1000 km, both the phase detection and event definition rate is significantly lower and Hagfors mainly picks up the larger events.

In Fig. 37 we have investigated the EP-processing event definition capability with respect to distance and magnitude. We see, as expected, that at shorter distances the Hagfors arrays identify most of the events (green and blue dots) and further away only the larger events are identified. It is, however, a little surprising that some of the very closest events go undefined in the EP-processing. We also see more clearly in Fig. 37 the lack of EP-defined events at some distances. Note that we have truncated the event distribution at 2000 km since Hagfors contributes very little beyond that distance.

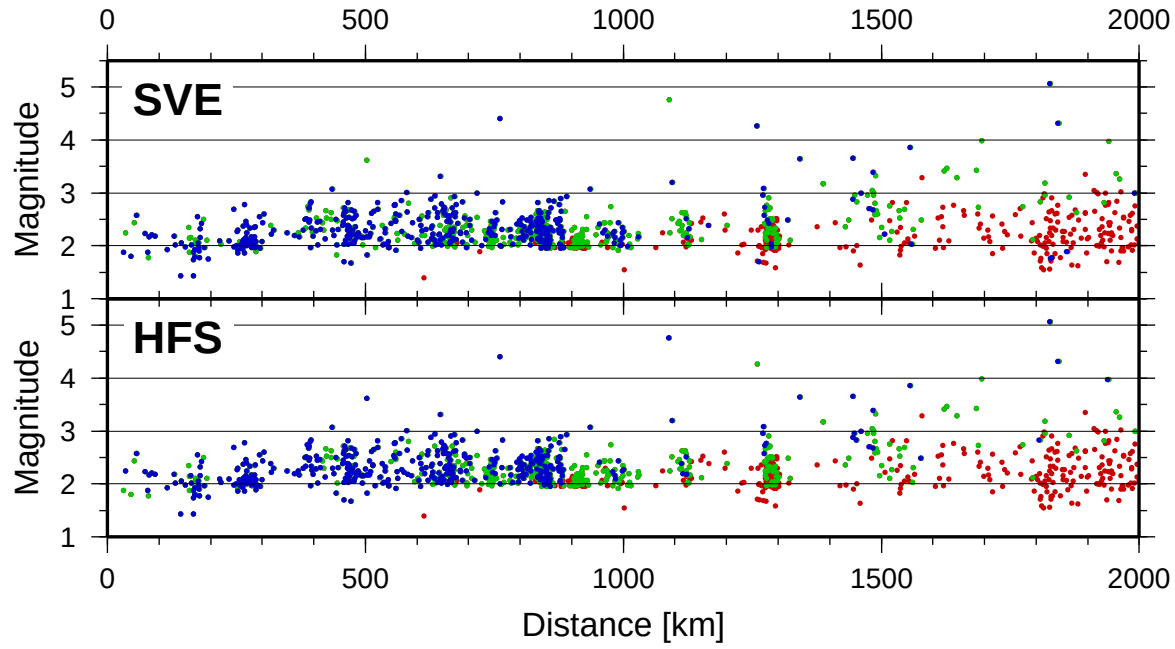

Figure 37: Plots of local magnitude vs. distance from the Hagfors arrays. The red dots show all the events in the NORSAR regional bulletin, the green dots are overlaid the red where there are Hagfors readings in the bulletin, the blue dots are events for which the single array EP-processing has defined an event. SVE) Results from the SVE array. HFS) Results from the HFS array.

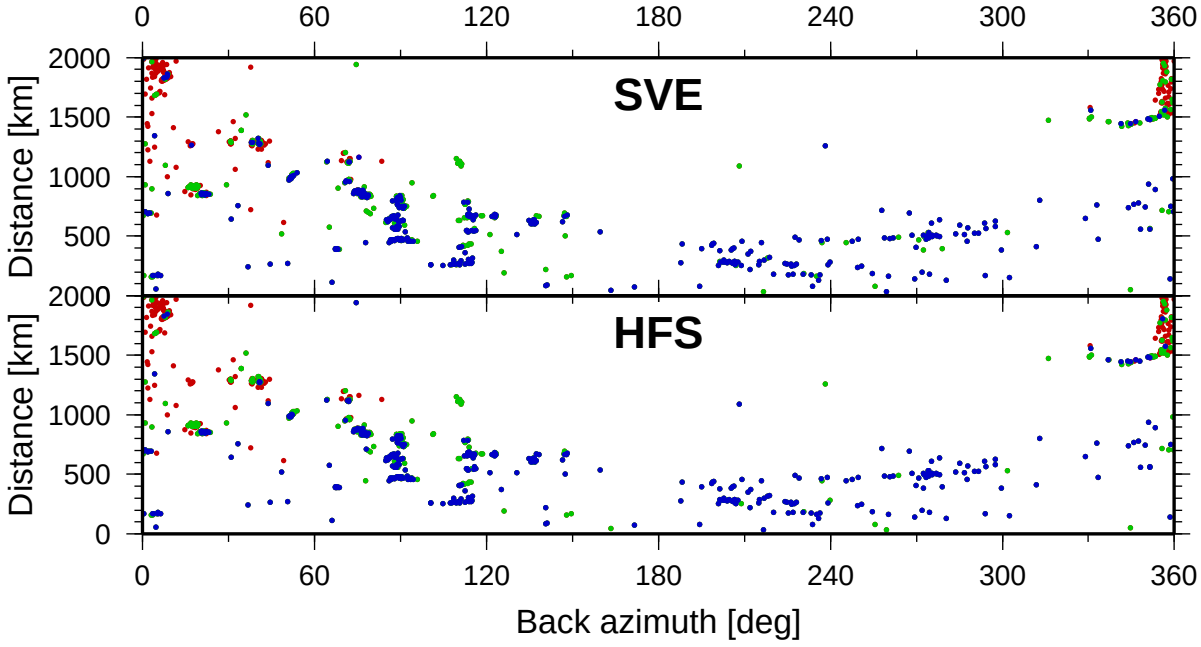

Figure 38: Plots of distance from the Hagfors arrays vs. back azimuth. The red dots show all the events in the NORSAR regional bulletin, the green dots are overlaid the red where there are Hagfors readings in the bulletin, the blue dots are events for which the single array EP-processing has defined an event. SVE) Results from the SVE array. HFS) Results from the HFS array.

Fig. 38 explores the azimuthal distribution of successfully EP-defined events, with distance. The figure shows clearly how Hagfors is in the southern part of the NRRB area of interest, there are very few events in the bulletin beyond 500 km south of Hagfors. We see that there is no azimuthal dependency of the EP identified events at the two arrays, what stands out in Fig. 38 is only the previously observed distance dependency. We also note, again, that the two arrays identify approximately the same events.

Estimation errors in the location process

In the sections below we will study the errors in the EP locations, for both arrays, as compared to the NRRB locations. We include all NRRB events that have EP definitions at the arrays, i.e. 464 events at SVE and 454 events at HFS. We will also highlight four clusters of events which have been well detected on both arrays in order to study azimuthal and distance dependent errors. The clusters are at Gällivare (67°N, 21°E) purple dots, Karelia (61°N, 29°E) green dots, western Norway (62°N, 4°E) yellow dots, and Göteborg (58°N, 12°E) red dots, see the map in Fig. 36. In the figures below we have denoted the median, mean and L2 standard deviation in order to have some simple, statistical measures of the distributions. We are, however, aware that some of the distributions do not resemble normal or exponential distributions, especially the skew apparent velocity residuals.

Azimuth residuals The azimuth residuals at array SVE and array HFS versus distance to the event, are shown in Fig. 39. We see that at both arrays the azimuth residuals are small for nearby events and grow rapidly for events out to approximately 300 km, after which they stay rather constant (except for the odd outlier). This observation, that the azimuth errors are rarely more than 30°, almost independent of the distance to the event is probably explained by the event association process. There is a cut off on how much the azimuth estimates of the different phases can differ from each other for an event to be defined. This cut off is frequently set to 30° (Schweitzer, personal communication) and is therefore likely to be causing the observed effect. Our four special areas show a similar azimuth residual pattern as the entire distribution, indicating

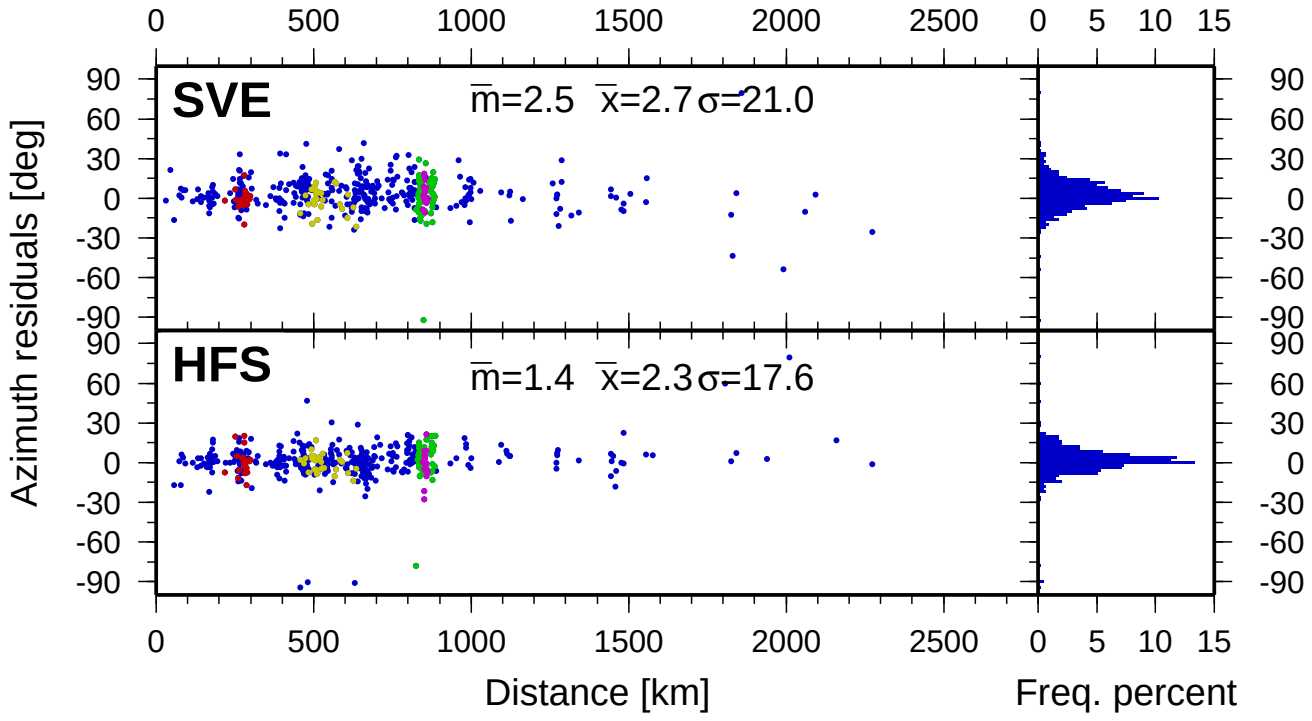

Figure 39: Plots of azimuth residuals vs. distance from the Hagfors arrays. $\bar{m}$ is the median, $\bar{x}$ the mean and σ the standard deviation of the residuals. The rightmost section of the plots shows frequency percent histograms of the residual distributions. SVE) Events defined at the SVE array. HFS) Events defined at the HFS array.

no azimuthal variation in the residuals. SVE has generally larger residuals than HFS, the standard deviation is 21° compared to 17.6° at HFS, and is also more offset from zero than HFS. This is surprising, considering

that SVE is the larger array with more instruments, but may be explained by the aforementioned bias in the NRRB due to its use of HFS data and the lack of processing optimization of the SVE array.

Apparent velocity residuals We show the apparent velocity residuals at SVE and HFS in Fig. 40. Most of these residuals are P wave residuals, but a small number of S wave residuals, 22 for SVE and 26 for HFS, are also present. The S wave residuals are generally more negative than the P wave residuals and, therefore, shift median and mean values to lower values. This shift is, however, small and less than 0.1°. The standard deviations are even less affected. As expected, the residuals are small for events close to the arrays and grow

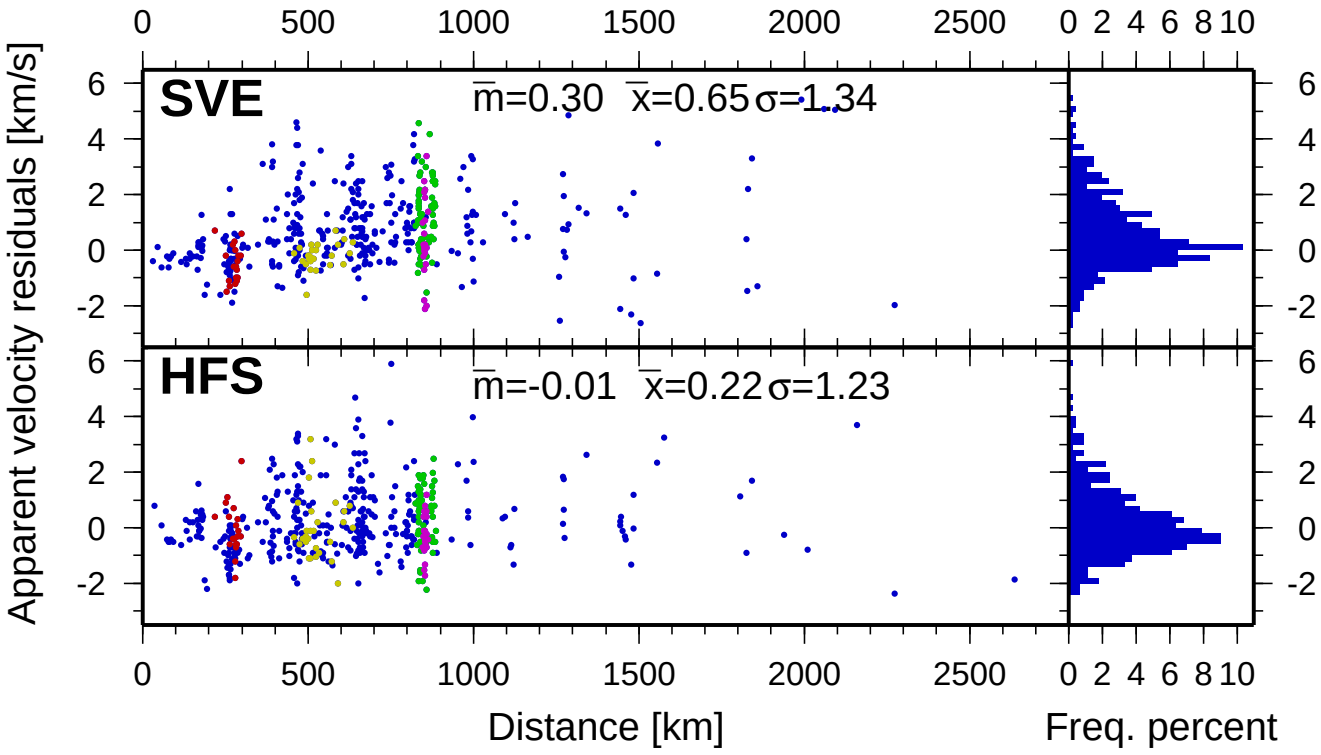

Figure 40: Plots of apparent velocity residuals vs. distance from the Hagfors arrays. $\bar{m}$ is the median, $\bar{x}$ the mean and σ the standard deviation of the residuals. The rightmost section of the plots shows frequency percent histograms of the residual distributions. SVE) Events defined at the SVE array. HFS) Events defined at the HFS array.

with distance. The residual distributions are skew, ranging from approximately -2 km/s to +4 km/s. This implies that the observed apparent velocities are generally higher than those calculated from the NORSAR model. Interestingly, up to a distance of approximately 300 km the residuals grow in the negative direction and there are relatively few positive residuals. After 300 km, however, the lower limit of negative residuals is set and the residuals immediately show a more positive character. The residuals for the Göteborg and western Norway groups have less variability than those from Gällivare and eastern Finland, and also less variability than the rest of the events. This is, however, most likely not a result of varying azimuthal properties east to west. The Göteborg group, at 250-300 km distance, have apparent velocity residuals that are very similar to those from a group outside of Stockholm, located at a similar distance from Hagfors but due east. Finally, we see that SVE again has higher standard deviation of the residuals than HFS. The apparent velocity residual distributions are, however, skew and the standard deviation is not the best measure of deviation.

Location residuals We have calculated the distances between the correct location of the events and the locations provided by the EP algorithm for the individual arrays, see Fig. 41. The figure shows that the location errors are very large and that the grow approximately linearly with distance from the arrays. Both arrays show an interesting "upper" line of very mis-located events, with location errors almost as large as the distances. Below these, the bulk of the residuals grow more slowly. Again, the SVE array has generally larger residuals than the HFS array.

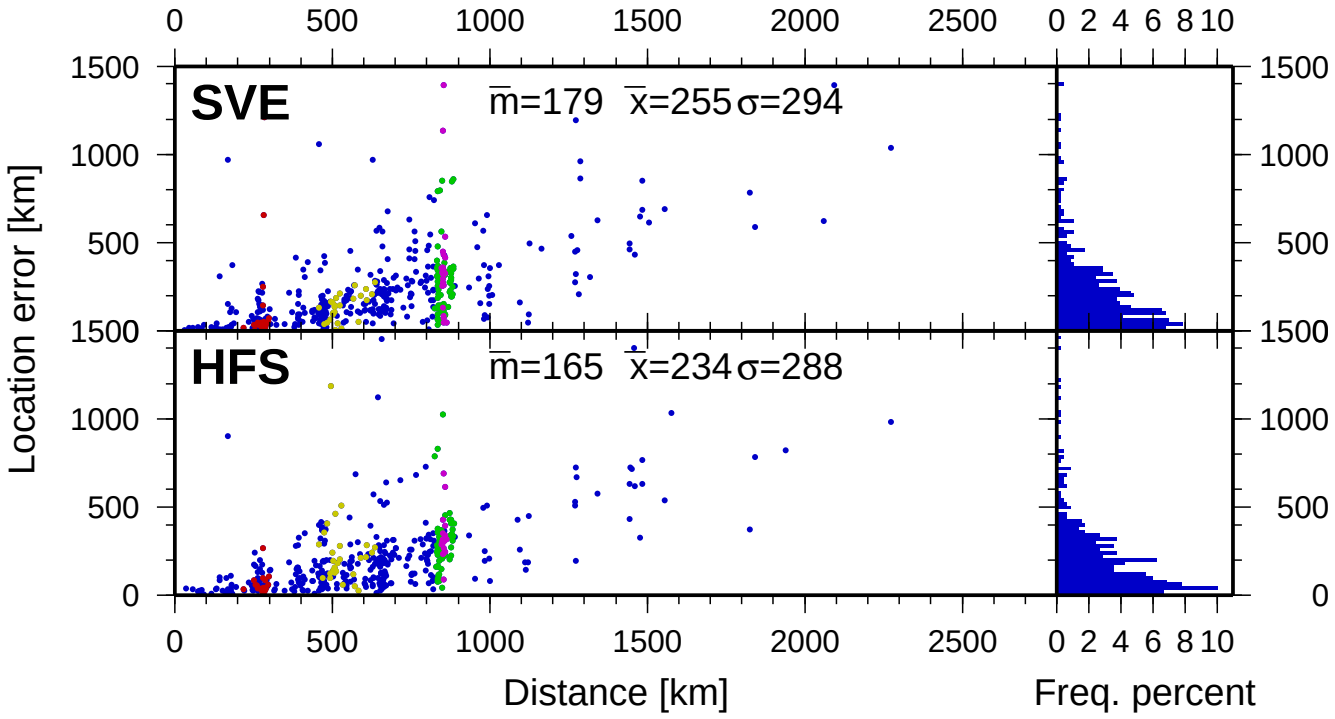

Figure 41: Plots of location residuals vs. distance from the Hagfors arrays. $\bar{m}$ is the median, $\bar{x}$ the mean and σ the standard deviation of the residuals. The rightmost section of the plots shows frequency percent histograms of the residual distributions. SVE) Events defined at the SVE array. HFS) Events defined at the HFS array.

In addition to the material presented here we have listed some specific issues with the EP processing in Appendix C. There are examples of phase identification, phase association and event definition mishaps in the processing.

5.2.3 Comparison with the SNSN bulletin

The Swedish National Seismic Network, operated by the Department of Earth Sciences at Uppsala University, recorded 374 earthquakes during the time of simultaneous operation of the two Hagfors arrays. Most of these events are below magnitude one, the median local magnitude is 0.46, which implies that many of them are not detected at Hagfors. The EP-algorithms defined 42 events at SVE and 35 events at HFS which fit with phase arrival times from events in the SNSN bulletin, see Fig. 42. For the processing of the SNSN data we have utilized the SNSN velocity model for Scandinavia [Slunga, personal communication].

We see that, as above, the EP processing at the two arrays find approximately the same events. Also, as with the NRRB events, EP at the new SVE array manages to identify more of the SNSN events than the HFS array. Seeing that so few of the SNSN events are seen at Hagfors, we will not present an in depth analysis as with the NRRB events above. Studying the events we conclude that most of the observations above are in agreement with the SNSN events, i.e. the residuals are generally a little poorer at SVE, there is no obvious azimuthal dependency (note however that from Hagfors most of the SNSN events are to the NE), azimuths are much more dependable than locations.

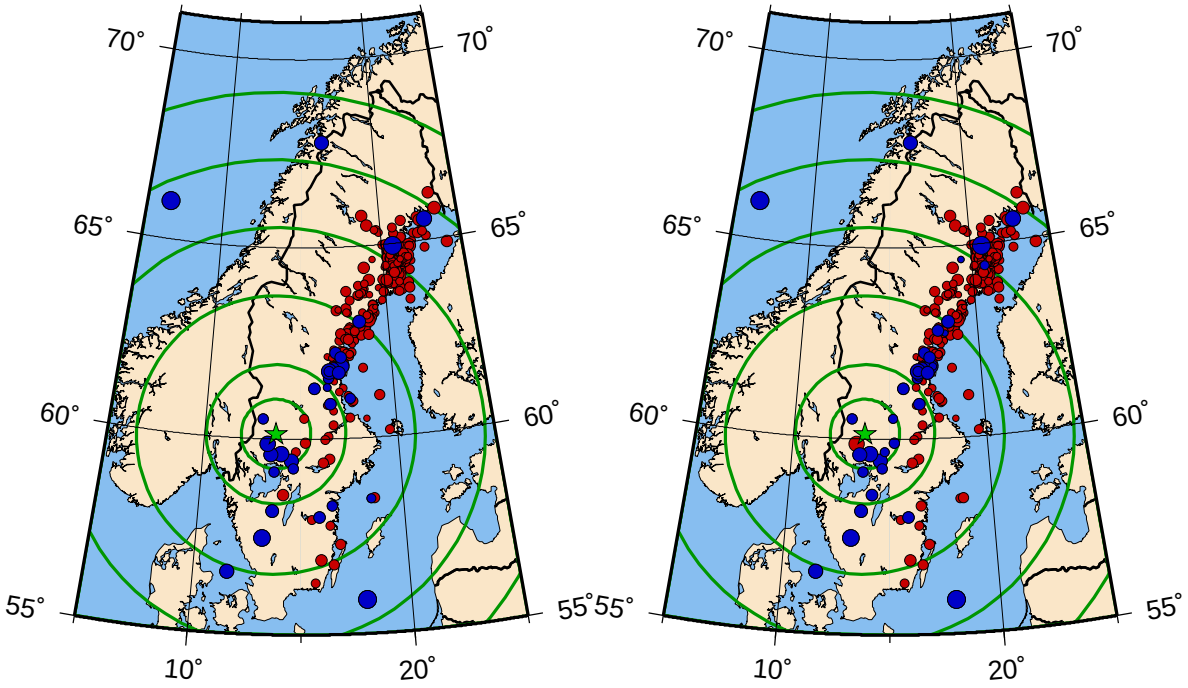

Figure 42: The red dots show the distribution of events in the SNSN reviewed bulletin for the time period 2/4-2002 to 21/9-2003. The Hagfors array is marked with a green star, green circles show distances of 100, 200, 400, 600, 800 and 1000 km from Hagfors. Left) Events identified by the HFS array in blue. Right) Events identified at the SVE array in blue.

5.2.4 Summary

The results of the study of single array station event location using the EP algorithms show that single array location in not a trivial matter. Comparing the single array locations at HFS and SVE with the NORSAR regional reviewed bulletin (NRRB) it is disconcerting to find that only approximately half of the events from HFS/SVE included in the bulletin, with enough phases to define an event, are actually defined in the EP processing. The main problem seems to be to associate a correct S phase with the identified P phase. Once defined, azimuth estimates to the events seem rather robust but distances are, again probably because of the S phase difficulty, notoriously problematic.

The detection level at SVE seems to be greatly enhanced as compared to HFS, many more events are defined (although many probably spurious) and the issue of an "event generator" due south of the Hagfors station might have gone unnoticed were it not for the detection capability of the new array. Unfortunately, in this study the excellent detection properties are not accompanied by equally high quality location properties. This is, however, as discussed above, most likely an effect of a less than optimal, non-tuned implementation of the EP software coupled with a bias from the use of the NRRB which was based partly on the old, HFS, array. The performance of the SVE array should therefore be optimized using the tools available in the EP-software and then validated using the NRRB, based on SVE data, and other high quality bulletins.

6 Software

During the course of the work reported here a number of pieces of software was developed in order to facilitate the analysis. Much of the work of the first sections were performed using Matlab, so Matlab scripts for noise and event spatial correlation are available, as are scripts for array gain analysis and general signal characteristics.

In order to parse and extract information from the various bulletins the following programs were developed. All these take the -h option for some helpful text.

readgbf.c C program that reads the daily, automatic NORSAR GBF (Generalized Beam Forming) files.

```
readgbf [-h] [-a lat1 lat2] [-b lon1 lon2] [-l location_string] [-m magn]
        [-n nstat] [-s stat] GBF_file(s)
The program searches through any number of GBF daily files, as specified
    on the command line, and prints events that meet the search criteria.
    One option has to be specified and all options have to go before
    the GBF files.

    -a Upper and lower latitude limits.
    -b Upper and lower longitude limits.
    -l String, within double quotes, with a geographic location.
    -m Lowest magnitude.
    -n Lowest number of stations.
    -s Specific station, e.g. SVE.

Björn Lund, Feb 2003
```

readREB.py Python script that reads daily Reviewed Event Bulletin files from the International Data Center at CTBTO in Vienna.

```
Extract event information from one or more REB files written in
the IMS1.0 format. All events are listed if no further
options are set. The script writes to stdout by default.

readREB.py [-h] [-c lat_s lat_n lon_w lon_e] [-m mag] [-n num]
         [-o output_file] [-r deg1 deg2] [-s num stat] [-x num] REB_file(s)

   Options:
     -c lat1 2 lon1 2 Latitudes and longitudes defining a box.
                      Def: -90 <= lat <= 90, South negative.
                      -180 < lon <= 180, West negative.
                      Always put the south coordinate before the north,
                      and the west coordinate before the east.
     -h               This text.
     -m mag           Smallest magnitude (mb) for extraction.
     -n num           Smallest number of defining stations for extraction.
     -o file          Name of output file, default is to stdout.
     -r deg1 deg2     Span of angular distance from the station, min and max,
                      default is 0 to inf.
     -s num stat(s)   Extract events where the num station(s) stat(s) has
                      reported.
     -x num           Output choice:
                         0) Everything.
                         1) All event info.
                         2) All station info.
                         3) Event coords for GMT.
                         4) Station azimuth and azimuth residual.
                         5) Station slowness and slowness residual.
                         6) Event numbers.

Björn Lund, September 2003
```

readEPX.py Python script that reads the daily, automatic NORSAR EPX files.

```
Extract event information from one or more EPX files.
All events are listed if no further options are set.
The script writes to stdout by default.

readEPX.py [-h] [-c lat_s lat_n lon_w lon_e] [-m mag]
   [-o output_file] [-r deg1 deg2] [-x num] EPX_file(s)

  Options:
    -c lat1 2 lon1 2 Latitudes and longitudes defining a box.
                     Def: -90 <= lat <= 90, South negative.
                     -180 < lon <= 180, West negative.
                     Always put the south coordinate before the north,
                     and the west coordinate before the east.
    -h               This text.
    -m mag           Smallest magnitude (ML) for extraction.
    -o file          Name of output file, default is to stdout.
    -r deg1 deg2     Span of angular distance from the station, min and max,
                     default is 0 to inf.
    -p SNR           Smallest P-wave SNR for extraction.
    -s SNR           Smallest S-wave SNR for extraction.
    -x num           Output choice:
                        1) All event info.
                        2) Event coords for GMT.
                        3) Distance [km] and back-azimuth.
                        4) Max amplitude P-wave LOCATE string.
                        5) Max amplitude S-wave LOCATE string.
                        6) Event numbers.

Björn Lund, December 2003
```

compEv.py Python script that goes through files from SNSN's bulletin or NORSAR's regional reviewed bulletin (html files) and tries to find the corresponding events in the EPX file lists.

```
Find events from the EPX processing also present in other
bulletins, such as the NORSAR regional, Uppsala etc.

compEv.py [-h] [-a array] [-e epx_path] [-o utfil]
          [-t type] [-v vel_mod] input_file(s)

  Options:
    -a arr     Array, HFS=1, SVE=2. Default = 1
    -b         Only write out a concise bulletin file.
    -e path    Path to the EPX year subdirectories. Default /dat/BULL/EPX/
    -h         This text.
    -o fil     Output file, default is epx_ut.dat.
    -t type    Bulletin:  1=SNSN events.lib 2=NORSAR regional reviewed (html).
               Default = 1
    -v mod     Velocity model. 1=SNSN, 2=NORSAR regional, 3=iaspei91, 4=PREM.
               Default = 1

Björn Lund, March 2004
```

readSeis.py Python module containing utility functions for the reading of different bulletins.

seis.py Python module for some more general seismology oriented functions, such as distance calculations on a sphere.

7 Summary and discussion

The upgraded Hagfors seismic array has more elements and is somewhat larger than the old array, it has modern instrumentation with higher sensitivity and a modern data acquisition system. It should, therefore, perform somewhat better than the old array. This study shows that the performance of the new array is, indeed, a little better than that of the old array. However, there are many factors beside the physical hardware that determines the quality of array performance.

We show in this report that resolution of the array in azimuth and slowness space is significantly improved with the new array. Noise investigations confirms that Hagfors is a very silent area, all of our instruments record noise close to the lower limit of the low noise model. The correlation of the noise shows the behaviour anticipated from the site investigation [1], i.e. large regions of intra-element spacings with negative correlation, which also confirms the expectations that the new array was constructed to optimize intra-array element spacings to distances of observed negative correlation.

Maximum array gain is improved, in theory, from $\sqrt{8} = 2.83$ to $\sqrt{10} = 3.16$ simply by the addition of two extra element sites. Studies of actual array gain, at different frequencies, in this report confirms that the gain of the new array is an improvement over the old array gain. Interestingly, we observe that the utilization of a large number of intra-array element spacings with negative correlation does pay off in terms of array gain. The new array frequently shows gain above the expected maximum gain. We note that negative noise correlation is seen in a rather wide band, between approximately 2 - 7 Hz, providing increased gain for a large range of teleseismic to local events.

The very clear detection at Hagfors of the 12.5 ton chemical explosion during the Kazakhstan field experiment shows that the station is very sensitive to events in the region. We show that the signal is clearly visible after ordinary bandpass filtering, beamforming is not even necessary.

As an auxiliary seismic station, Hagfors data is requested by the IDC on an event basis. We have shown how Hagfors data today, after an upgrade of the IDC auxiliary station request software, is utilized in a more consistent manner than before and that Hagfors has detections on more than 77% of the Reviewed Event Bulletin (REB) events within 30°. The change from the old to the new array in the IDC processing on December 17, 2002, significantly improved the azimuth and slowness residuals of the Hagfors detections, but also shifted the median residuals slightly off the correct/model values. This tendency toward higher precision, but less accurate residuals needs to be further investigated and, if proven correct, should be taken into account in the processing by the implementation of phase/azimuth/region dependent array corrections.

We show that the automatic single array locations at the Hagfors arrays did not work satisfactorily during the studied time period. A large number of events is defined, the new array defines approximately 2.5 times more events compared to the old array, many of these are probably spurious but the main problem is that large events with well detected phases are not correctly located. We found a large number of events due south of Hagfors, detected mostly on the new array, which have locations from Hagfors to northern Italy. This is probably a local noise source, perhaps the steel works in Uddeholm, which should be further investigated. Of the 857 events in the NORSAR regional reviewed bulletin with Hagfors phases, most of the events above magnitude 2, only approximately half are correctly identified as events by the automatic event processing (EP). The events' phases are correctly detected but the association of phases to events is troublesome. Even relatively close events with large magnitudes are sometimes missed. We recommend that more resources are directed toward an enhancement of the single array location process. It would be advantageous for FOI to have relatively reliable single array locations, both locally, regionally and world wide, in its role as a National Data Center.

Acknowledgments

We thank Johannes Schweitzer and Ulf Baadshaug at NORSAR for always answering our questions and supplying us with a wealth of data. We also thank Tormod Kværna at NORSAR for helping with the array response. Florian Haslinger and Peder Johansson at the CTBTO's IMS and IDC patiently tracked down IMS and IDC related information for us, thank you. Thanks to Nils-Olov Bergkvist at FOI for the analysis of the Kazakhstan event in section 4.3. Nils-Olov Bergkvist, Ragnar Slunga, Dan Öberg and Leif Persson at FOI assisted with ideas, Hagfors knowledge and information and Matlab knowhow. We analysed many events using NORSAR's EP software and many of the figures in this report were produced using the open-source software GMT [7].

References

[1] Lund B., N-O. Bergkvist and P. Larsen, Report 1, Element Locations, Sub-Surface Vault Design and Cable Specifications in the Upgrade of Auxiliary Seismic Station AS101, Hagfors, Sweden, FOI-01-2532, FOI, Stockholm, Sweden, 2001.

[2] Bähler, S., Studies of Noise and Signals from The Hagfors Sub-Array for Array Configuration Design, FOA Rapport C 20757-9.1, FOA, Stockholm, Sweden, 1989.

[3] Mykkeltveit, S., K. Åstebøl, D.J. Doornbos and E.S. Huseby, Seismic array configuration optimization, Bull. Seis. Soc. Am., **73,** 173–186, 1983.

[4] Schweitzer, J., J. Fyen, S. Mykkeltveit and T. Kværna, Manual of Seismological Observatory Practices, Chapter 9, Seismic Arrays, NORSAR, Kjeller, Norway, 2001.

[5] Mykkeltveit, S. and F. Ringdal, Phase identification and event location at regional distance using small-aperture array data., in *Identification of seismic sources - earthquake or underground explosion*, Eds. E.S. Husebye and S. Mykkeltveit, 467-481, NATO Advanced Study Institutes Series C, D. Reidel Publishing Company, Dordrecht, Holland, 1981.

[6] Crotwell, P.H., T.J. Owens and J. Ritsema, The TauP toolkit; flexible seismic travel-time and ray-path utilities., Seis. Res. Lett. **70**, 154-160, 1999.

[7] Wessel, P. and W.H.F. Smith, New, improved version of the Generic Mapping Tools released, EOS Trans. AGU, **79**, 579, 1998.

Appendices:

A Sensitivities for sensors and digitizers in the new and the old array

Site	Seismometer	Seismometer sensitivity (V/m/s)	Digitizer sensitivity (nV/count)	Preamplifier gain (dB)
HFA0	GS-13	2000	2538	29.61
HFA1	GS-13	2000	2508	29.61
HFA2	GS-13	2000	2560	29.61
HFA3	GS-13	2000	2562	29.61
HFB1	GS-13	2000	2582	29.61
HFB2	GS-13	2000	2569	29.61
HFB3	GS-13	2000	2544	29.61
HFB4	GS-13	2000	2564	29.61
HFB5	GS-13	2000	2565	29.61
HFC2	STS-2	1500	864	-

Table 6: Sensitivities for sensors and digitizers in the new array

Site	Channel code	Seismometer	Seismometer sensitivity
HFSA1	shz	S-13	0.02655 nm/count @ 1 second
HFSB1	shz	20171A	0.02623 nm/count @ 1 second
HFSB2	shz	20171A	0.03068 nm/count @ 1 second
HFSB3	shz	S-13	0.02866 nm/count @ 1 second
HFSB4	shz	S-13	0.02929 nm/count @ 1 second
HFSB5	shz	S-13	0.02394 nm/count @ 1 second
HFSC1	shz	20171A	0.02561 nm/count @ 1 second
HFSC2	shz	S-13	0.025 nm/count @ 1 second
HFSC2	shn	S-13	0.025 nm/count @ 1 second
HFSC2	she	S-13	0.025 nm/count @ 1 second
HFSC2	lhz	7505A	0.34544 nm/count @ 20 seconds
HFSC2	lhn	8700C	0.32524 nm/count @ 20 seconds
HFSC2	lhe	8700C	0.35787 nm/count @ 20 seconds
HFSC2	bhz	STS-1V	0.006 nm/count @ 1 second

Table 7: Sensitivities for sensors and digitizers in the old array

B Hagfors REB events for various regions

For reference we include REB events for four additional regions of the world during the time period January 1, 2000 to October 12, 2003. The maps below show both all REB detected events in the regions and the events which had Hagfors contributions. These maps give some insight into the current event rate and REB detection ability in the regions.

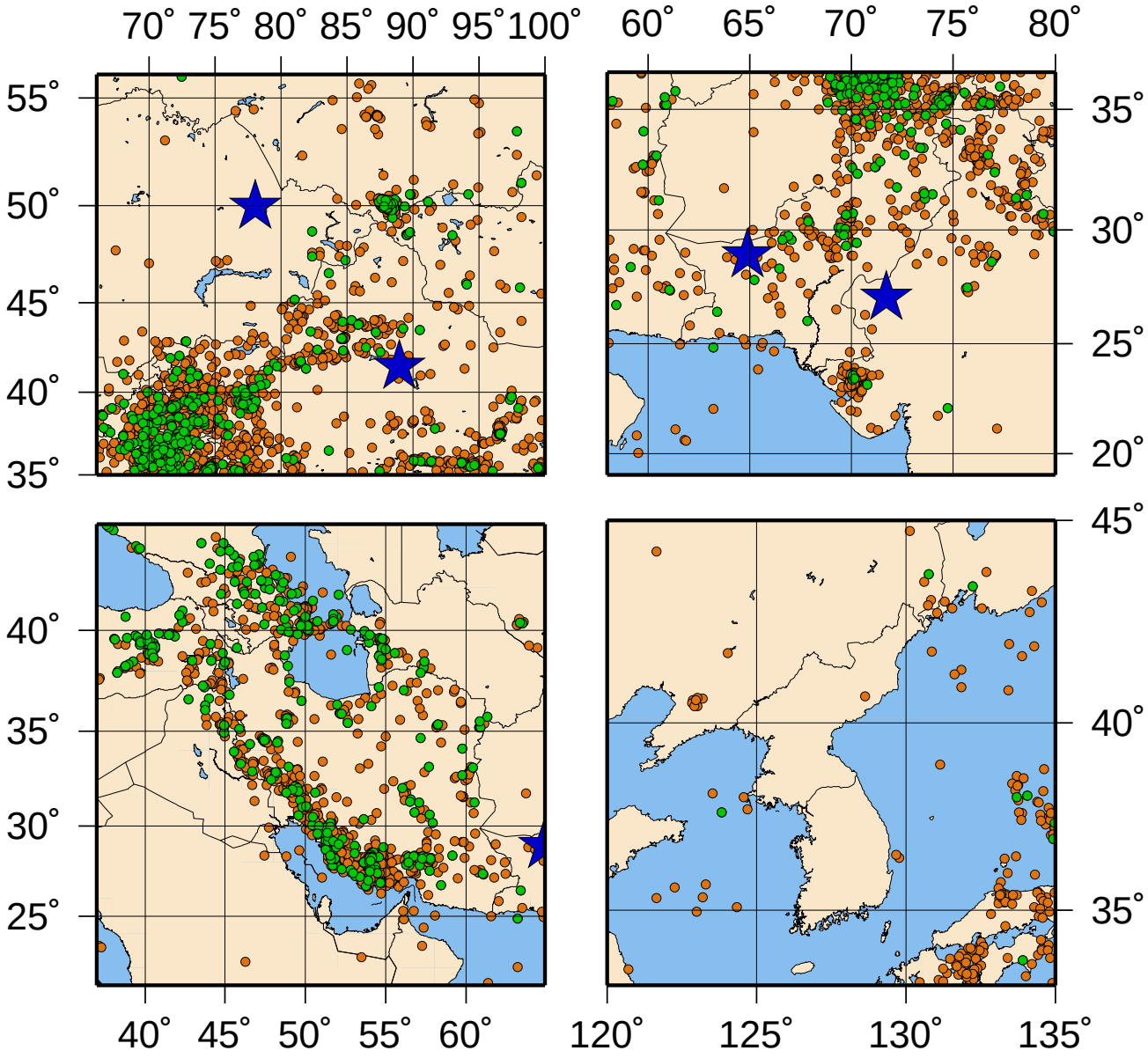

Figure 43: Orange dots are all events in the REB, green dots are events where Hagfors contributed. Blue stars are nuclear test sites. A) Semipalatinsk (Kazakhstan) and Lop Nor (China) test sites. 531 events with Hagfors contribution, 2919 total in the REB. B) Pokhran (India) and Chagai (Pakistan) test sites. 244/1595 events. C) Iran/Iraq. 302/1176 events. D) Korean peninsula. 8/175 events.

C EP-processing issues

During our work with the EP-processing we found a number of problems with the phase identification and association procedures. We will list two examples from the EPX-files below (for an explanation of the EPX-file entries, see [4]), and also point to the south of Gotland event of December 18, 2002, with origin time (OT) 21:14:25.16 and magnitude 3.61 according to the NRRB and OT 21:14:19.83 and magnitude 3.32 according to the SNSN bulletin. This event was not identified on SVE because the major, well detected, Pn phase was ignored. Subsequent minor phases were associated to two different events. On HFS, the event was correctly defined and reasonably well located.

EPX file entries are as follows. Two lines declare an event, the HYP and EPX lines. The EPX line contains event number, OT, latitude, longitude, ML, distance in km, back-azimuth and fixed depth (0F). Following is associated phases; ID number, arrival time, station code, phase name, max. amplitude in nm, corresponding dominant frequency in Hz, the SNR, the beam name, apparent velocity, back-azimuth and an explanatory code. LOCATE means the phase was used for location, ASSOC means it was associated but not used for location. Tele means interpretation as a teleseismic phase, Noplot3ci means not used for event definition. See also page 48-49 of +citech9.

The first example shows a missed S phase at the old HFS array which ruins the distance estimate to the array. Compare the location error between the HFS and SVE arrays:
OT: 2002 5 10 7 43 36.230000 Lat: 58.558 Lon: 10.492 Mag: 2.30

HFS02130.EPX

```
   330                HYP 536 VAERMLAND REGION SWEDEN
   330 130:07.44.03.5 EPX          59.661   12.597 1.04      80.9 229.6   0F
915866 130:07.44.13.1 HFS PN        4.923  6.1   186.1 HB23   8.8 224.8 LOCATE
915867 130:07.44.18.0 HFS PN        7.394  6.0    18.4 HF13   7.6 228.4 ASSOC
915868 130:07.44.19.0 HFS PN        8.473  6.1     7.7 HD01   8.1 226.4 ASSOC
   330 130:07.44.20.0 MAG ML        6.876  5.7  2054.0 aVG    4.9 229.6 LOCATE
915869 130:07.44.23.4 HFS PG        3.786  6.2     6.9 HC21   7.4 230.2 LOCATE
915870 130:07.44.24.9 HFS LG        4.067  5.7     8.2 HD24   5.0 231.1 LOCATE
915871 130:07.44.27.9 HFS S         3.055  3.9     4.2 HH02   5.9 232.4 ASSOC
915873 130:07.44.48.0 HFS SG       19.931  3.5    14.2 HF14   3.4 231.6 Unassoc
915876 130:07.44.53.6 HFS SG        8.126  5.3     8.4 HF20   4.2 208.3 ASSOC
915874 130:07.44.54.0 HFS SG        9.557  5.2    18.1 HH02   4.0 209.9 ASSOC
915877 130:07.44.55.7 HFS RG        7.304  1.5     4.2 HA03   3.0 221.3 Unassoc
915878 130:07.44.57.2 HFS SG        7.649  3.6     4.8 HF16   3.3 222.4 ASSOC
```

The location routine does not use the large SG phase but puts the event much too close due to the misinterpreted LG and S phases. Location parameters are:
Az diff: 2.190100 Loc err: 171.690757 km; P_t diff: -0.300000
Vp_app diff: 0.597728 S_t diff: 7.440000 Vs_app diff: -1.339961

Same event on SVE is SVE02130.EPX

```
 14570                HYP 536 SKAGERRAK
 14570 130:07.43.39.1 EPX          58.585   10.702 4.99     241.7 225.6   0F
915886 130:07.44.13.2 SVE PN     4051.300  7.4   175.5 SA23   8.7 227.8 LOCATE
915890 130:07.44.14.9 SVE PN     3640.100  7.3    15.6 SF16   8.1 226.7 ASSOC
915893 130:07.44.19.5 SVE PN     4881.600  7.5     8.3 SE07   8.6 229.3 ASSOC
915895 130:07.44.22.1 SVE PG     1541.800  5.5    10.4 SE12   6.5 222.1 LOCATE
915898 130:07.44.25.4 SVE PG     1514.600  6.4     4.7 SA24   6.7 236.4 ASSOC
915901 130:07.44.29.0 SVE PG     1557.300  7.4     3.2 SH03   7.5 211.5 ASSOC
915912 130:07.44.47.5 SVE SG     11337.20  4.9    18.8 SH02   3.7 225.5 LOCATE
915915 130:07.44.48.3 SVE SG     6884.800  3.2    12.7 SF20   3.6 227.2 ASSOC
915918 130:07.44.53.7 SVE SG     10277.00  4.6    15.2 SC12   4.1 223.9 ASSOC
915919 130:07.44.54.2 SVE SG     10601.80  4.5     9.9 SF10   3.5 228.6 ASSOC
 14570 130:07.44.55.0 MAG ML     7827.665  4.9  7827.7 aVG    3.2 225.6 LOCATE
915921 130:07.44.57.4 SVE SG     4650.500  3.8     5.9 SF18   3.8 219.3 ASSOC
```

Here the correct phase is identified and the event is more or less correctly located.

Az diff: -1.809900 Loc err: 12.540646 km; P_t diff: -0.200000
Vp_app diff: 0.497728 S_t diff: 6.940000 Vs_app diff: -1.039961

Sometimes there are large errors in the EP-processing, this is SVE and a magnitude 2.3 close by. Theoretical arrivals:
OT: 2003 9 2 12 20 58.531000
Phase, TT, ArrT, Slowness:
P: 6.48, 2003 9 2 12 21 5.01, 0.165032826693
S: 11.15, 2003 9 2 12 21 9.68, 0.284504002158

SVE03245.EPX

```
751730 245:12.19.19.3 SVE SG        0.800  3.9     6.5 SH02   3.8 240.1 Plot3ci
751758 245:12.21.05.4 SVE PG      278.204 11.7  5670.0 SH04   6.7 219.6 Plot3ci
751760 245:12.21.16.0 SVE nois     36.780  5.2     4.8 SB16   1.1 216.1 Plot3ci
751759 245:12.21.14.0 SVE RG       36.391  5.0     7.9 SF19   1.8  33.1 Noplot3ci
751761 245:12.21.19.4 SVE SG       46.994  7.3     2.7 SH03   3.5  53.8 Noplot3ci
751797 245:12.31.15.8 SVE SG        1.309  3.7     5.7 SH02   4.2 236.2 Plot3ci
```

We see that the P arrival is in the phase detection list, with very high signal to noise, but there has not been an event declared. This is similar to the above mentioned south of Gotland event. Conversely, on HFS:

HFS03245.EPX

```
   150                HYP 536 VAERMLAND REGION SWEDEN
   150 245:12.20.53.3 EPX          59.659   12.791 2.60       0.0   0.0   0F
   150 245:12.21.04.2 MAG ML      251.250  5.2 69331.5 aVG    6.7 223.8 LOCATE
751736 245:12.21.05.2 HFS PG      439.757  8.4  5397.6 HC32   7.0 219.2 LOCATE
751737 245:12.21.14.2 HFS LG       49.336  5.2     8.5 HE12   4.3 224.9 LOCATE
751738 245:12.21.16.1 HFS nois     23.997  4.4     4.6 HA09   2.0 209.3 ASSOC
```